MODELING, FABRICATION AND OPTIMIZATION OF OPTICALLY TRANSPARENT – THERMALLY INSULATING SILICA AEROGELS FOR SOLAR THERMAL APPLICATIONS

BY

AHMET ALPEREN GÜNAY

THESIS

Submitted in partial fulfillment of the requirements
for the degree of Master of Science in Mechanical Engineering
in the Graduate College of the
University of Illinois at Urbana-Champaign, 2016

Urbana, Illinois

Advisor:

Assistant Professor Nenad Miljkovic

ABSTRACT

Solar thermal energy conversion has the potential to reduce greenhouse gas emissions via the offset of fossil fuel burning power generation methods. By capturing the suns energy and using it to heat steam as part of a Rankine cycle, electrical energy can be renewably produced. Furthermore, solar thermal collectors have high potential for domestic heating when deployed at the rooftop scale, reducing fossil fuel consumption used for home heating needs. The efficiency of these solar applications is highly dependent on the ability of the collecting device to absorb the incoming solar energy, and minimize thermal losses to the environment. Current techniques utilize vacuum tubes to eliminate convective losses, in combination with selective surfaces (high absorptivity in the solar spectrum, and low emissivity in the infra-red (IR)) to minimize thermal re-radiation. Here, we present an alternate approach that operates at atmospheric pressures with simple, black, absorbing surfaces. An Optically Transparent Thermally Insulating (OTTI) layer was assumed to be coated on the back side of the black, broadband absorber. This absorber was assumed to have perfect transparency and opacity in the solar spectrum and Infra-Red (IR), respectively. In order to provide a deeper understanding of the link between the optimum OTTI layer material properties and the overall solar thermal efficiency, we developed a coupled radiative-conduction heat transfer (HT) model used to predict how the investigated OTTI layers will behave when they are used as solar thermal absorbers. The optimum properties that were obtain were then incorporated into the HT model to study the thermal performance under various optical concentrations (1 – 20 suns), solar thermal absorber temperatures (20 – 200°C), and external heat transfer coefficients (10 – 100 W/m^2K). The results showed potential solar thermal conversion efficiencies of ≈90% can be attained by utilizing OTTI layers as insulators in the solar thermal absorbers. To check if a material to have the assumed material properties can be fabricated, silica aerogels were procured, synthesized and characterized. Due to their naturally high and low transmissivities in the solar and IR spectrums, respectively, silica

based aerogels coated on the back with highly absorbing (black) surfaces offer a potential solution to create simple and inexpensive solar thermal absorbers. To test our hypothesis, we fabricated tetramethyl orthosilicate (TMOS) and tetraethyl orthosilicate (TEOS) based silica aerogels. The formed gels were aged for 3 weeks and dried using a carbon dioxide supercritical point dryer. The obtained aerogel optical properties were characterized using ultraviolet-visible (UV-Vis) and Fourier Transform Infrared (FTIR) spectroscopy, showing spectrally averaged ($0 < \lambda < 2.7$ μm) transmissions of ≈87% for a sample thickness of 4mm. To minimize the effect the O-H group transmission reduction occurring in the solar spectrum, we modified the baseline aerogels to be hydrophobic with a silane treatment to shield the exposed hydroxyl groups on the surface. Hydrophobic modification resulted in an increase of the spectrally averaged transmissions to ≈ 94%. This study sheds light on the applicability of silica aerogels on black coatings as ideal solar thermal absorbers and offers insights into new avenues for performance improvement of solar thermal energy systems.

ACKNOWLEDGMENTS

I would like to thank the Mechanical Science and Engineering Department at University of Illinois for providing me with the opportunity to conduct research and undergo graduate studies with them. I would like to graciously thank Professor Quinn Brewster for his help and guidance on the radiation work I performed over the past two years.

The spectroscopy and particle size analyses were carried out in part in the Frederick Seitz Material Research Laboratory Central Research Facilities, University of Illinois. The supercritical drying of the aerogels was performed in the Beckman Institute for Advanced Science and Technology, University of Illinois. I would like to thank Mark Bee for his support in the drying process.

Most importantly, I would like to express my sincere gratitude to my advisor, Professor Nenad Miljkovic, for his care, understanding and guidance. I could not have done anything I achieved in this work without his support. I would also like to thank my lab mates in the Energy Transport Research Lab for their support. Especially, I would like to thank Mr. Jesus Sotelo, Mr. Michael Atten, Mr. Naveen Nagarajan and Mr. Mateusz Lopez for their help in performing the aerogel research.

Finally, I would like to thank my girlfriend, İrem, my brothers, İlteriş and Kutalmış, and my parents, Nejla and Mehmet. Without their support, I could not have been standing where I am now.

TABLE OF CONTENTS

LIST OF SYMBOLS

λ	Wavelength
OTTI	Optically Transparent Thermally Insulating
PV	Photovoltaic
DLS	Dynamic Light Scattering
UV-Vis	Ultra Violet – Visible
FTIR	Fourier Transform Infra Red
TMOS	Tetramethyl Orthosilicate
TEOS	Tetraethyl Orthosilicate
DCCA	Drying Control Chemical Additive
TMCS	Trimethyl Chlorosilane
HMDS	Hexamethyl Disilazane
$t_{p,i}$	time for i'th purge (min)
$t_{se,i}$	time for i'th solvent exchange (min)
V_{gel}	Volume of the gel (mL)
V_{eth}	Volume of the ethanol (mL)

C_i	i'th constant
ρ_{gel}	Density of the gel (g/mL)
m_{gel}	Mass of the gel (g)
Me	Methanol
Et	Ethanol
$I_{b\lambda}$	Spectral Blackbody Intensity (W/(m^{2}srμm))
h	Planck's Constant
c_0	Speed of Light
T	Temperature (K)
q_{rb}	Total Blackbody Flux (W/m^2)
k_b	Boltzmann's Constant
σ	Stefan-Boltzmann Constant
I_λ	Spectral Intensity (W/(m^{2}srμm))
e_Ω	Unit vector in the Ω Direction
$K_{e\lambda}$	Spectral Extinction Coefficient (1/m)
$K_{a\lambda}$	Spectral Absorption Coefficient (1/m)

$K_{s\lambda}$	Spectral Scattering Coefficient (1/m)
$p_\lambda(\Omega' \rightarrow \Omega)$	Phase Function for scattering from Ω' to Ω
μ	Direction Cosine
Ω_s	Solid Angle of the Sun
τ_λ	Spectral Transmissivity
α_λ	Spectral Absorptivity
ε_λ	Spectral Emissivity
G_C	Solar Concentration Factor
T_∞	Ambient Temperature (K)
q_r	Radiative Flux (W/m^2)
k	Thermal Conductivity (W/mK)
U	Overall Heat Transfer Coefficient, bottom (W/m^2K)
U_{top}	Overall Heat Transfer Coefficient, top (W/m^2K)
η	Conversion Efficiency
ρ	Density (kg/m^3)

H	Specific Enthalpy (J/kg)
P	Pressure (Pa)
Φ	Viscous Dissipation (J/m^3)
N	Total number of Species
i	Index
$\dot{q}$	Volumetric Heat Generation (J/m^3)
Y_i	Mass fraction of the i,th species
V_i	Velocity of the i,th species (m/s)
h_i	Specific Enthalpy of the i,th species (J/kg)
T_{bot}	Temperature of the Bottom Surface (K)
T_{bot}	Temperature of the Top Surface (K)
ΔT_{bot}	Difference in Temperature for the Bottom Surface (K)
ΔT_{top}	Difference in Temperature for the Top Surface (K)

CHAPTER 1: INTRODUCTION

The need to convert to renewable energy is increasing day by day, with the oil and coal reserves getting drained at tremendous speeds and with the threat of global warming due to increased air pollution levels that are caused by traditional power plants. In order to save our world, researchers have looked into many methods of renewable energy; such as solar, wind power and hydro. The main problems of these techniques are that the efficiencies of the power plants utilizing renewable energy resources are not as high as the traditional petroleum or coal based facilities. Therefore, tremendous amounts of effort are taken in order to improve the efficiencies of these power plants.

The sun is the sole source of life and energy of our world. It is always radiating at the same intensity, which is what the earth makes use of to support life on its surface and beyond. Although the sun is an endless source of energy, it is not that trivial to harvest that energy for our needs. In fact, the most widely used forms of solar energy are the least efficient amongst the other top candidates for renewable energy with the current technologies, and the ones that do compete are expensive and hard to sustain [1]. Therefore, solar energy harnessing has to be developed into a much better technology in order to use the vast energy that the sun's rays carry, which can be achieved by making use of optimum insulation techniques that can be cost effectively built and implemented.

The solar radiation is mainly concentrated on the lower wavelength regimes, such as the Ultra- Violet, Visible and the Near Infra Red regimes ($0 < \lambda < 2.7$ μm)[2]. Therefore, the insulating material should not block the light that is coming in from the sun for these specific wavelength regions. On the other hand, the radiative losses from the surfaces that account for the low efficiencies happen in the middle Infra Red regimes ($2.7\ \mu m < \lambda < 20\ \mu m$) for low to moderate temperatures ($300\ K < T < 900\ K$). Thus, if the insulating material can block the lights from getting out in these regimes, a heat trap will be created and the

losses will be minimized due to the fact that the trapped heat will be emitted or conducted back to the absorbing surface.

Ideally, an insulating material must also have low thermal conductivity in order to minimize the thermal losses. Thus, a material that has favorable optical and thermal characteristics must be found, or developed. Silica aerogels are promising candidates for these purposes due to their favorable and adjustable optical properties, and their low thermal conductivities. While low thermal conductivity of silica aerogel limits conductive losses from the material that it is insulating; its optical properties might also allow it to let sunlight pass through and block the emitted rays from the material that it is insulating. Therefore, it can trap the heat that would normally be lost without proper insulation. Hence, silica aerogels have the potential to replace any material or technique that is currently used for the insulation of solar systems [3, 4, 5].

This chapter is devoted to investigating the current technologies that are being employed, with their advantages and drawbacks. Furthermore, the motivation and the scope of the study are also given here.

1.1. Background

This study includes both numerical and experimental aspects. The numerical aspect of the study is devoted to finding the optimum solar insulation characteristics and simulating the material with these characteristics in a numerical model to inspect how the material functions. This will then enable the scientists to localize their attentions on the materials that possess those physical traits. The second aspect of the study is devoted to the fabrication and characterization of the silica aerogels, which are considered to be one of the best candidates for optimum solar insulation.

1.1.1. Current Solar Insulation Techniques

Although there are many possible methods to make use of sun's rays in a thermal system, the mainly utilized two techniques are using Photovoltaic (PV) cells and Solar Thermal technologies [6, 7]. Only these two prominent techniques will be discussed here in detail.

One striking fact that is realized while studying the current solar insulation techniques is that their thermal efficiencies are usually around 30%, unless an expensive and complex design is used to increase it to a higher value. These low efficiencies usually stem from the emissivity losses. The energy of a photon has a quartic dependence on temperature, and therefore increased temperatures increase the losses significantly [8]. Thus, the main problem to be addressed in a solar absorbing system is to limit emissive losses, while increasing the absorption of the solar radiation.

1.1.1.1. Photovoltaic (PV) Cells

PV devices convert solar energy directly into electricity by utilizing the photovoltaic effect. Photovoltaic effect is a physical phenomenon observed in semiconductors that can be defined as the creation of an electrical driving force such as current or voltage through exposure to light [9]. Some portion of the energy that is carried by light is absorbed by the semiconducting material, and this energy excites the electrons that are attached to the semiconductor, causing them to become free. Then, these electrons can be induced to travel in a specific circuit, which in turn sends electricity to the power system [10]. A schematic of a PV cell is given in Figure 1-1. A Schematic of a Photovoltaic Cell [11].

This technique is a very sustainable way to harness solar energy. However, although the fabrication techniques were made easier and more cost effective through decades, these systems are limited to a maximum efficiency of 33.7%, which is called the Shockley-Queisser limit [12]. Some ways to surpass this limit

have been showed by scientists through years; however, these methods include cascading of a number of PV's together and/or using different semiconductors with complex designs [13]. Therefore, these methods to surpass the limits and improve the efficiency are not cost effective and not widely utilized.

1.1.1.2. Solar Thermal Technologies

The second most prominent way to harvest solar energy is using solar thermal technologies. In this method, sun's rays are incident on a highly reflective surface with a specific design, which concentrates all the rates to an absorbing surface. This surface usually has a working fluid inside which gets heated by the absorbed radiation. The hot fluid is then fed into a thermodynamic cycle such as the Rankine cycle to generate electricity [14]. Since the surface of the absorber typically gets very hot, the emissivity losses are tremendous and without proper insulation, the efficiencies are limited to about 40%. A schematic of a parabolic trough collector, which is the most widely used solar thermal technology globally, is given in Figure 1-2. A Schematic of a Solar Thermal System [11].

One way to increase the thermal efficiency of a solar thermal system is to make use of a vacuum tube. In this approach, the air surrounding the pipe is sucked out by the use of a sealed glass with specific connections in order to obtain a vacuum environment. This way, the convective losses are minimized due to the evacuation of the moving fluid surrounding the hot surface [15]. However, this gives no advantage on the emissive losses, since light does not need a medium to travel [16].

In order to atone for that, researchers have developed selective surfaces. In these surfaces, the front of the material is textured through a specific, complex design, which aims at trapping the low energy photons and directing them back to the system. The emissive losses ideally consist of photons that have much lower energies than the solar rays; thus, trapping lower energy ones and directing them back to the surface decreases the emissivity of the system drastically. At

the same time, these surfaces are designed in a way to let as many of the solar rays pass into the system as possible in order to maximize absorption. In order to maximize the selectiveness, these systems usually consist of cascaded absorbers with a textured front [17]. These systems can achieve effective absorptivities up to approximately 95% and effective emissivities as low as 5% [18].

In order to make the insulation even better, selective surfaces are used together with the vacuum tubes; so that both emissive and convective losses are minimized [19]. However, due to the presence of the glass in the system, the effective absorptivities go down to about 80% due to added reflection as well as the absorption in the glass. Although these systems work great, they have a lot of drawback. First of all, they require very complex designs to make them and scientists spend a very long time to even make them. Second, their fabrication costs are very expensive. Finally, keeping these surfaces and maintaining a good vacuum environment over the years is a very big issue. Therefore, scientists have been seeking for better solutions for decades in order to find a better and cheaper insulation for solar systems.

1.1.2. Silica Aerogels

Aerogels are mesoporous materials that are composed of a network of interconnected nanostructures and that possess very high porosities [20]. The first aerogel came to be in 1931, when Samuel Stephens Kistler made a bet with a friend claiming he could replace the liquids inside the jellies with a gas without shrinking them. The resulting material was called aerogel. A lot of research has been performed on the aerogels due to the tunability of their material properties. In fact, the lowest density and thermal conductivity materials that have been recorded were all aerogels [20, 21]. Through the years, a number of materials including aluminum, carbon, et cetera have been used in aerogel production; however, the most commonly used material for making aerogels is silica.

Silica is an insulating material, which is the oxide of silicon. Since it is an insulating material, its thermal conductivity is low (k = 1.4 W/mK). When used in aerogel form, though, its thermal conductivity becomes ultra low (k ~ 0.05 W/mK). Therefore, silica aerogels have been used in insulation for a few decades. They also have favorable and adjustable optical characteristics for solar insulation.

Silica aerogels have been used in various fields such as electronics, space programs and energy systems [22]. Even the National Aeronautics and Space Administration (NASA) utilizes them quite extensively in the form of dust collectors for their space programs due to their low weight and ultra insulation properties, and has a big laboratory devoted to aerogel research in the Glenn Research Center in Ohio [23]. It is because of the same properties of the silica aerogels that a lot of research has been performed on the development of them; and therefore, the silica aerogels are very promising candidates to be used as the optimum insulation for various fields, including renewable energy.

1.2. Motivation and the Proposed System

In this section, the motivation of the study is given. Moreover, the system that is proposed in order to optimize and improve the solar absorbers is also presented.

1.2.1. Motivation

The main motivation behind pursuing this study is to find how effective optimum insulation will be in terms of thermal efficiency improvements for solar thermal absorbers. This will be performed by modeling a thin sheet absorbing black surface that has a material with optimum insulation characteristics placed on top of it. The optimum insulation characteristics are obtained through the use of an optically transparent thermally insulating (OTTI) material. The results will then be compared to no insulation and vacuum chamber-selective surface insulation cases.

Beyond the optimization, the silica aerogels will also be investigated for their optical properties, densities and particle size distributions; and the effects of these parameters to their insulation capabilities will be discussed. Therefore, another motivation of this study is to find the properties of the silica aerogels that would lead to optimum insulation for solar energy harnessing purposes. These silica aerogels then replace the complex insulating techniques mentioned in Section 1.1.1 to reduce cost and complexity.

1.2.2. Proposed System

The proposed system includes the use of an OTTI material of sufficient thickness. The material will directly be mounted on the broadband absorber of any kind, which eliminates the complexity of the design. The insulating material will have a very high transmissivity to solar radiation ($\tau \approx 1$), and will also have a very high emissivity ($\varepsilon \approx 1$). In other words, the material will absorb the majority of the low energy photons. That way, while all the solar rays are passed through the absorber, the low energy photons that are emitted by the solar absorber will be absorbed by the insulator and will be conducted and emitted back to it, creating a heat trap to increase thermal efficiency.

For the insulating material, it is proposed to use OTTI silica aerogels in this study. Silica aerogels not only have very low thermal conductivities, but they also have tunable optical properties and can be made very transparent to solar radiation if the fabrication process is optimized. Moreover, their emissivities are also usually very high. Therefore, the insulator for this proposed work is an optimized silica aerogel with a very high optical transmissivity.

A schematic of the proposed system is given in Figure 1-3. A Schematic of the Proposed Solar Energy Harnessing System

1.3. Scope of the Research

In this section, the limitations, the unique aspects, and the potential impacts of the study are given in detail.

1.3.1. Limitations of the Study

Due to time limitations, the thermal part of the study is purely numerical. The numerical model will include the material which possesses optimum insulation properties, namely perfect transmission for solar spectrum ($0 < \lambda < 2.7$ μm), and perfect absorption for emission spectrum ($\lambda > 2.7$ μm). A single, average thermal conductivity of k = 0.005 W/mK will be used for the optimum insulator. Moreover, the thickness of the OTTI layer that is to be modeled is assumed to be 4 mm. This number was chosen since the prepared aerogels were usually made to that thickness in the laboratory. Moreover, since the proposed model can work with any broadband absorber, a thin sheet black absorber has been modeled in order to minimize conductive resistance effects inside the absorber. Furthermore, the numerical model does not include the modeling of the fluid that is flowing inside the system. Instead, a constant mean temperature of the fluid with an average total heat transfer coefficient is assumed for the purposes of this study. A schematic of the optimum spectroscopic properties are given in Figure 1-4. The Normalized Intensities of the Sun (left) and the OTTI Layer (right) versus Wavelength. The Optimal Transmissivity Fraction is also given (left). The cut-off wavelength is 2.7 μm. In this figure, the blackbody intensities of the sun and the layer were normalized by their respective maximum values. Additionally, a sketch of the system to be modeled including the used parameters for the numerical model is depicted in Figure 1-5. Schematic of the OTTI Integrated Solar Thermal Absorber with Modeling Parameters

After the silica aerogels have been prepared, their optical properties will be investigated to see how close they are to optimum insulation. The thermal conductivity and porosity of the prepared aerogels will not be investigated due to

time limitations, as well. Instead, the densities and the particle size distributions will be analyzed in order to have an idea about the latter two.

1.3.2. Unique Aspects

This project investigates the possibility of using an OTTI layer for solar thermal insulation. With these OTTI layers, any kind of absorber can be insulated to decrease the thermal losses from the system significantly. With the design of the OTTI layers, the complexity in the design of selective surfaces and vacuum tubes is decreased. Moreover, the cost of creating and employing an insulating system also decreases drastically, making this system more practical and desirable. Finally, the OTTI layers also induce a heat trapping effect on the thermal emissive losses from the absorbing surface, making the solar energy harnessing systems more efficient.

1.3.3. Impact of the Study

The modeling part of the study will cover an ideal, optimum insulator on top of a black broadband absorber of any kind. Since the proposed system does not require a complex absorber of any kind, it might effectively replace the current technologies due to the reduced complexity and cost of the absorbing system. Moreover, any material that can be fabricated to the needs of optimum insulation can be used in the same model; so the model is not limited to silica aerogels, which is the considered optimum insulating material for this study.

Moreover, since silica aerogels are very good insulators with tunable properties, they can be utilized in a variety of scientific fields. The fabrication and optimization process is given in detail in this study; therefore, the recipes here can be modified for the insulation needs of any system. Furthermore, since the densities of silica aerogels are also considered here; systems that are not exposed to strong external forces, which also require low density materials in their designs, can also make use of the low density silica aerogels developed here.

1.4. Overview

The thesis consists of several chapters in order to distinguish different sections that contribute to different aspects of the study. Chapter 2 addresses the state-of-the-art technologies in solar insulation and aerogel fabrication through a literature survey. Chapter 3 discusses the theoretical background behind the existence of silica aerogels. Moreover, it also gives theoretical background on heat transfer analysis by dividing them into only radiation and coupled conduction and radiation analyses. Chapter 4 talks in detail about the fabrication procedures of the aerogel. Moreover, it also talks about the characterization of the aerogel by explaining some experimental techniques. Chapter 5 reviews the results that are described in the previous chapters. It also includes the discussions on which results are important and why. Chapter 6 summarizes the findings in Chapter 5 and concludes the thesis.

1.5. Figures

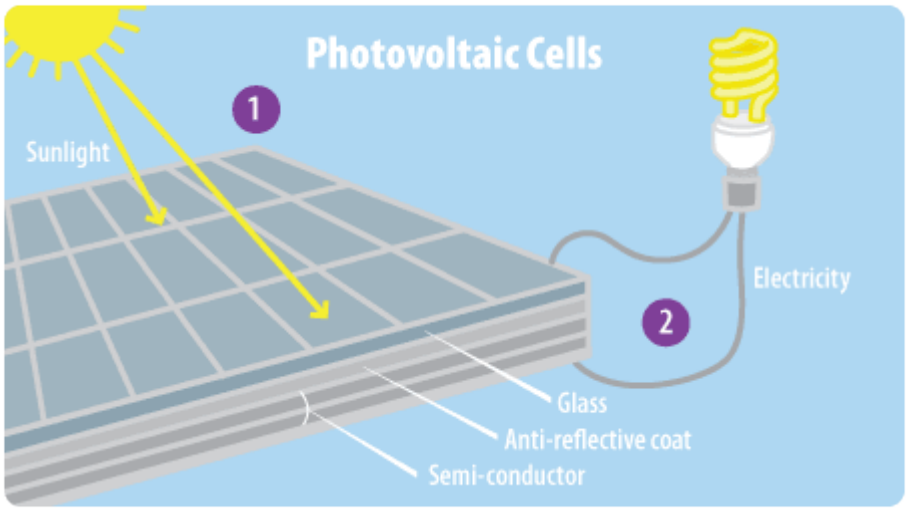

Figure 1-1. A Schematic of a Photovoltaic Cell. Adapted from Ref [11].

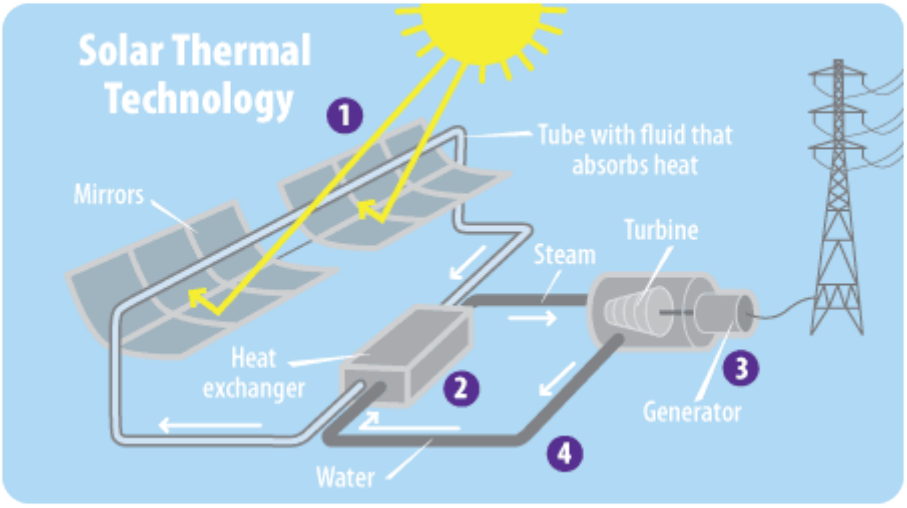

Figure 1-2. A Schematic of a Solar Thermal System. Adapted from Ref [11].

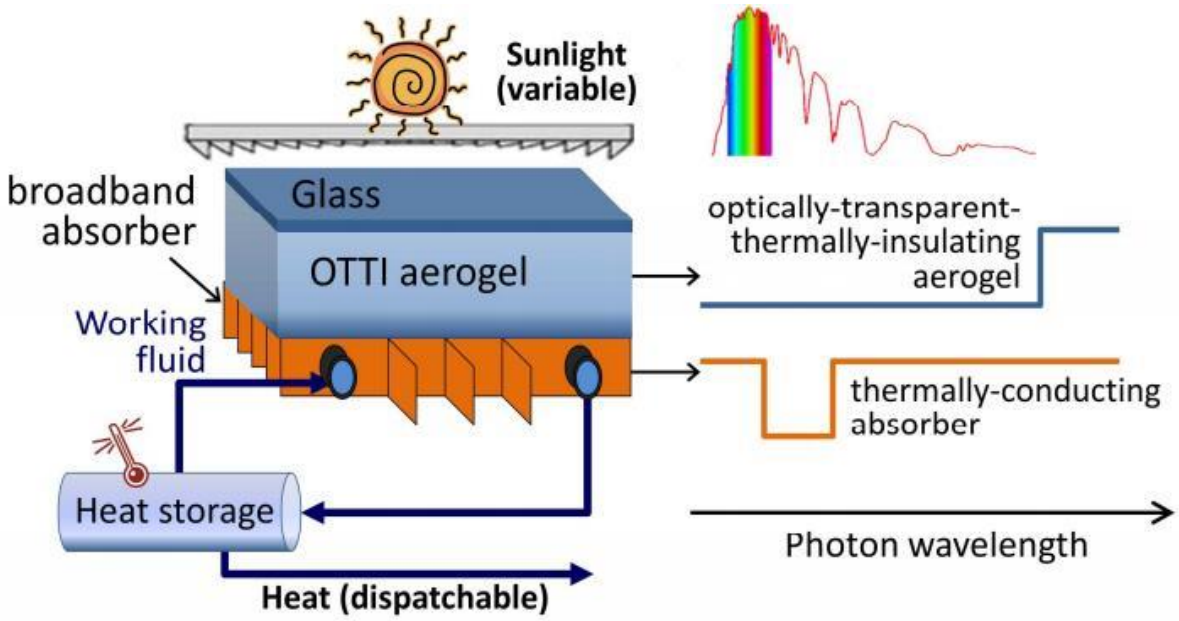

Figure 1-3. A Schematic of the Proposed Solar Energy Harnessing System

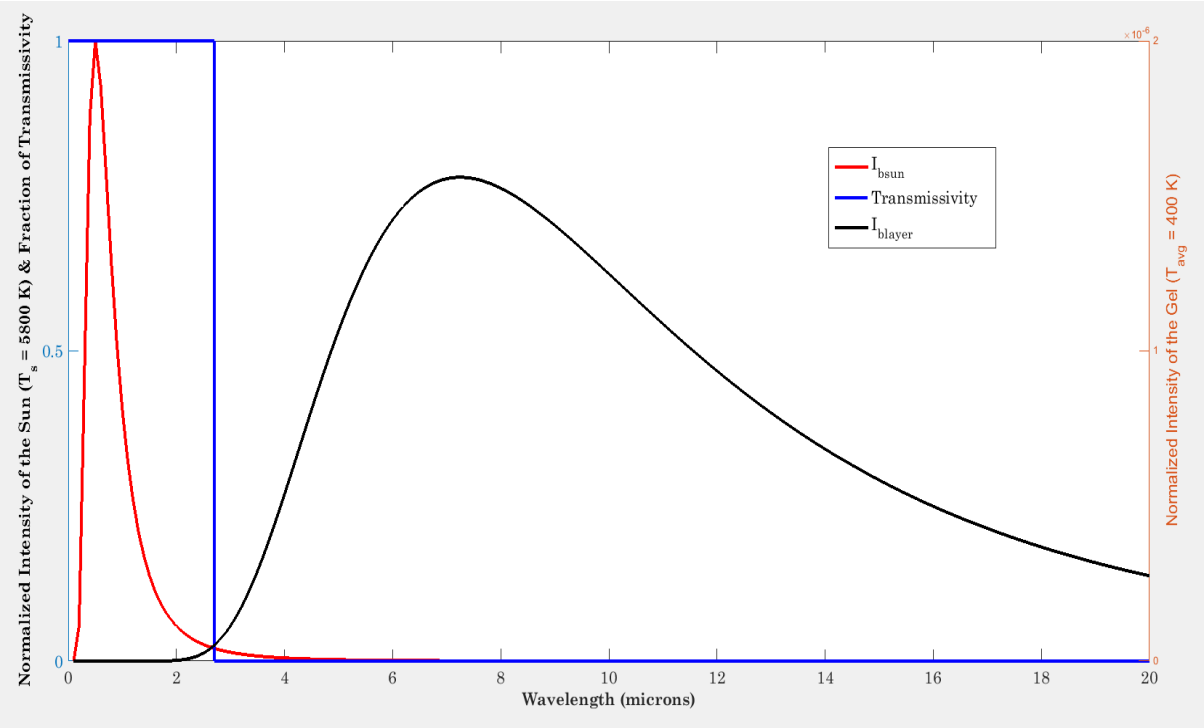

Figure 1-4. The Normalized Intensities of the Sun (left) and the OTTI Layer (right) versus Wavelength. The Optimal Transmissivity Fraction is also given (left). The cut-off wavelength is 2.7 μm.

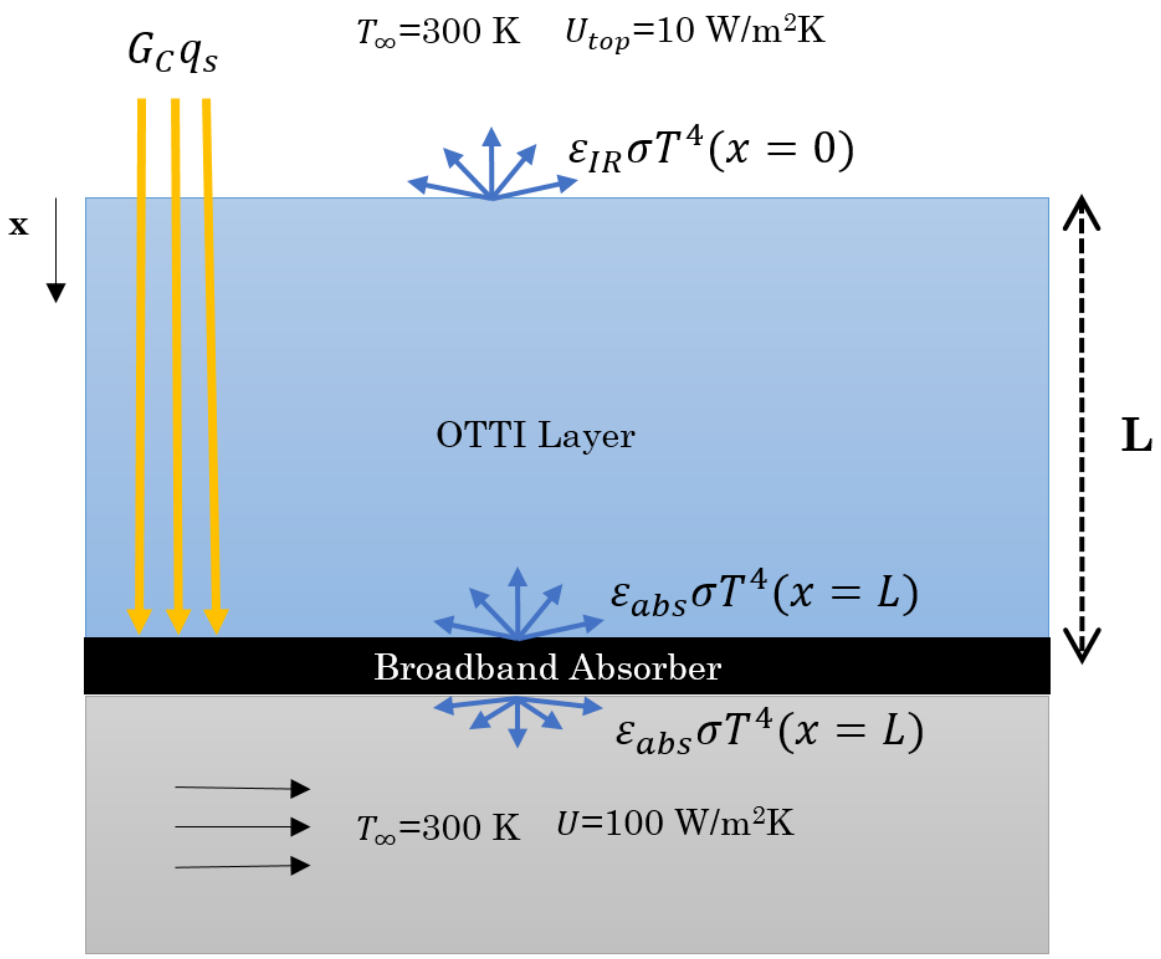

Figure 1-5. Schematic of the OTTI Integrated Solar Thermal Absorber with Modeling Parameters

CHAPTER 2: LITERATURE REVIEW

The use of optically transparent and thermally insulating (OTTI) materials have been thought of and implemented for solar thermal insulation [24]. The properties that the materials should have have been investigated and discussed [25, 26]. However, finding a material to exhibit this behavior perfectly was a challenge and thus researchers mainly tended to improve the selective surface technologies.

Researchers realized that aerogels could be used for solar insulation as early as two decades ago, and started performing research in this area [4, 5, 27]. Although their findings showed a potential, the obtained efficiencies were still below that of vacuum tube and selective surface technologies. The fabrication techniques of aerogels were also not developed sufficiently; thus, this area has been left in the shades other than a few studies, as well.

The production of aerogels, though, has been studied extensively [28, 29, 30, 31]. These studies show that in order to get an aerogel, a silicate source is diluted to obtain the sol-gel form, which later goes through deliquification to reach its final state. The silicate source can be anything; however, the speed of the reaction and the number of products after the reaction will change significantly depending on the choice of the source. These studies also note the volume shrinkage from the first sol-gel that is obtained when the final aerogel product is obtained. It is also mentioned in these papers that aerogels can be made from any material. They do not necessarily have to be made of silica. However, silica is chosen due to its low thermal conductivity and favorable optical properties.

Aerogels have a variety of applications including thermal, electrical and optical [32, 33]. Their low conductivities make them perfect for thermal insulation [34].The thermal conductivities of the aerogels can be made so low that the losses from the body under insulation can be considered almost negligible with further

optimization [35]. The electrical conductivities of the aerogels can be changed. While silica aerogels are not conducting electricity, organic aerogels may. The optical properties of aerogels are perhaps the most widely differing characteristics of the aerogels. While organic aerogels are usually black and absorbing, silica aerogels are usually transparent. However, the levels of transparency can also be further adjusted by tuning the recipes. A silica aerogel might even be opaque to solar radiation depending on the recipe. It is this tenability that makes aerogels materials of interest.

The most important stage of aerogel fabrication is the drying process. Usually, freeze drying or supercritical drying is utilized in order to avoid the cracks initiated due to the vapor liquid meniscus in the gel. Since the solid structure of aerogels are usually weak, the meniscus should be avoid in order to ensure that the surface tension forces do not collapse the solid matrix, creating cracks or fractures. One of the most important discoveries was to use the carbon dioxide supercritical drier to dry the aerogels [36]. The critical point temperatures of the alcohols are much higher than that of carbon dioxide; therefore, drying the alcohols supercritically was a huge problem. Here, it is showed that the alcohols can be mixed and replaced with carbon dioxide inside the aerogel, and then it will be enough for the gel to get past the critical point of carbon dioxide, rather than the respective alcohol. This was a huge discovery and now carbon dioxide supercritical driers are the prominent drying methods to synthesize aerogels.

However, there is still some research going on in the field of drying of aerogels. It was also showed that the aerogels can be dried inside ionic liquids subcritically, without having the need to get past the critical point [37]. The aerogels can also be made hydrophobic in order to decrease the effect of surface tension on the surfaces [38]. This allows for the aerogel to be dried subcritically when the evaporation rates and water contents are carefully controlled [39].

After the fabrication of the aerogels, their optical properties have to be characterized in order to verify that the synthesized gels can be used for solar thermal insulation. The optical properties to be measured include but are not limited to the refractive index, the absorption coefficient and the scattering efficiency [40]. After verifying the absorption coefficient and the scattering efficiencies are both low in the wavelength range of interest, it can be concluded that the gel is transparent to the spectrum of interest [41]. As mentioned previously in this study, the transparencies of the aerogels are tunable.

Although the aerogels are materials of high capacity and they are also sometimes called as one of the materials of the future, their production methods are still not sufficiently developed. Owing to that, aerogels cannot be found as commercial materials in the market. This is mainly due to the fact that the fabrication process of the aerogels usually includes supercritical drying and the aerogels are usually weak material which can easily be broken into pieces. In order to rectify for the weakness and brittleness, some research have been performed to make the aerogels stronger [42]. Moreover, since the aerogels are perfect insulators and have other cool properties, people have also been trying to make the aerogels commercially available [43].

CHAPTER 3: THEORY

The applicability of silica aerogels as an insulation material should be chemically and physically justified. The way to do that is to look at the theory and model it accordingly. This chapter will shed light on the chemistry behind the aerogels; specifically, why the aerogels form and what their chemical compositions are will be investigated. Furthermore, a physical theory on the heat transfer applications will be given. The solution of the physical theory will form the basis of the devised model of this study.

3.1. Chemical Theory

Here, only the chemical compositions of the TMOS and TEOS based aerogels will be considered. The chemical composition of TMOS and TEOS are $Si(OMe)_4$ and $Si(OEt)_4$, respectively. Here, Me represents methanol and Et represents ethanol. Then, when these substances react with water in an acidic or basic environment, silica particles are formed. The general chemical forms are shown in Equations *(3-1)* and *(3-2)* for TMOS and TEOS, respectively. Here, there are also insignificant amounts of some other chemicals produced, which are not shown in any of these equations.

$$Si(OMe)_4 + H_2O \xrightarrow{H\ or\ OH} SiO_2 + MeOH \qquad \textbf{(3-1)}$$

$$Si(OEt)_4 + H_2O \xrightarrow{H\ or\ OH} SiO_2 + EtOH \qquad \textbf{(3-2)}$$

The final form of the alcogel that mainly consists of SiO_2 and EtOH usually also has some amount of water due to the fact that the gelation process is usually not perfectly chemically balanced. Therefore, usually the alcogels have to be dehydrated using a pure alcohol to remove all the remaining water in the gel solution.

The pH levels of the environment that this reaction takes place also affect the chemical compositions and characteristics of the aerogels [39]. Nevertheless, for the purposes of this study, they were not investigated.

3.2. Heat Transfer Theory

Heat transfer can be defined as the thermal energy in transit due to a spatial temperature difference [44]. Since the application of the silica aerogels will include insulation for solar energy harnessing, heat transfer is the most important consideration. This is due to the fact that whether the utilization of aerogels as insulators will be significantly helpful in efficiency improvements for solar energy harnessing can solely be estimated by solving the total heat transfer model.

The heat transfer model will include two main parts for the purposes of this study. The first part will cover the radiative heat transfer, in which the solar beams that are incident on the solar thermal absorbing system are considered as well as the emissions from the surface and the surroundings. The second part will address the heat equation in which radiation and conduction can be coupled with specific boundary conditions.

3.2.1. Radiative Heat Transfer

Radiation is basically electromagnetic radiation emitted by particles that undergo internal energy state transitions [45]. Depending on the number of particles and their internal energy states, their radiative powers will be different. Electromagnetic waves do not need a medium to transfer; therefore, radiation from the sun comes directly onto the earth without being affected too much. The spectral intensity for a blackbody that is emitting radiation is given by Equation *(3-3)*. This distribution is also known as Planck function.

$$I_{b\lambda} = \frac{2hc_0^2}{\lambda^5(e^{\frac{hc_0}{k_b\lambda T}} - 1)} \qquad \textbf{(3-3)}$$

In the Planck function, there are some physical constants appearing. These numbers are Planck's constant h=6.626*10^{-34} (m^{2}kg)/s, speed of light c_0=2.998*10^8 m/s, and Boltzmann's constant k_b=1.3806*10^{-23} (m^{2}kg)/(s^{2}K). Heat transfer engineers are mainly interested in the flux, which will simply be the integration of the intensity field in all the directions. Since the blackbody radiation is isotropic, the spectral integration only yields a factor of π for the total blackbody intensity. Making use of these facts, the total blackbody flux is given by Equation *(3-4)*.

$$q_{rb} = \int_0^\infty \pi\, I_{b\lambda} = \sigma T^4 \qquad \textbf{(3-4)}$$

In Equation *(3-4)*, the σ is a constant called the Stefan-Boltzmann constant and σ=5.67*10^{-8} W/(m^{2}K^4). If these calculations are performed using these equations for the sun's temperature of T=5800 K, after geometric calculations, it is seen that the flux that is incident on the earth is 1360 W/m^2. However, the atmosphere reflects and absorbs some of this heat, letting only an average of approximately 340 W/m^2 pass. Nonetheless, for scientific considerations, scientists took the reference flux as 1000 W/m^2 and named it as a unit of 1 Suns.

After the intensities that will be incident upon the surfaces are found, the radiative heat transfer analysis for the combined solar absorbing system must be performed. The model will include a semitransparent material that is placed on top of a black body.

The radiative intensity field for any participating media is given by the Radiative Transfer Equation. The Transfer Equation is given in Equation *(3-5)*.

$$e_{\Omega}\nabla I_{\lambda}(\Omega) = -K_{e\lambda}I_{\lambda}(\Omega) + K_{a\lambda}I_{b\lambda} + \frac{K_{s\lambda}}{4\pi}\int_{4\pi} I_{\lambda}(\Omega')p_{\lambda}(\Omega' \to \Omega)d\Omega' \qquad \textbf{(3-5)}$$

where e_{Ω} is a unit vector in the Ω direction, $K_{e\lambda}$, $K_{a\lambda}$ and $K_{s\lambda}$ are the spectral extinction, absorption and scattering coefficients, respectively. Moreover, $p_{\lambda}(\Omega' \to \Omega)$ is the phase function for the change of direction due to scattering from the Ω' direction into the Ω direction. If this equation is further examined, it is seen that it handles the rate of change in the intensity in the medium, the emission from the medium, the incident intensity and the scattered rays. In fact, the scattered part is what makes this equation an Integro-Differential Equation without a closed form solution. Therefore, this equation either has to be numerically solved, or some other approximations have to be made. For instance, if scattering is not relevant, the equation becomes an ordinary differential equation, which is analytically solvable.

For the optimization purposes of this study, it is assumed that the rays in the solar spectrum are perfectly transmitted and the other rays are blocked. Thus, there is no scattered intensity and hence, the transfer equation that is left can be solved. The final form of the Transfer Equation is given in Equation *(3-6)* [46].

$$\mu\frac{dI_{\lambda}}{dx} = K_{e\lambda}(I_{b\lambda} - I_{\lambda}) \qquad \textbf{(3-6)}$$

where μ is the direction cosine, which is assumed to be 1 for the purposes of this study. μ=1 means the solar radiation is directly incident on the surface. The boundary conditions for the optimization solution are given in Equation *(3-7a)*.

$$I_\lambda(x=0,\mu) = 0.73\Omega_s\tau_\lambda G_C I_{b\lambda}(T=5800K)\frac{\delta(\mu-1)}{2\pi} + \varepsilon_\lambda I_{b\lambda}(T(x=0))\ 0 \le \mu \le 1 \qquad \textbf{(3-7a)}$$

$$I_\lambda(x=L,\mu) = \varepsilon_\lambda I_{b\lambda}(T(x=L))\ 0 \ge \mu \ge -1 \qquad \textbf{(3-7b)}$$

where L is the thickness of the insulator, Ω_s is the solid angle, τ_λ is the spectral transmissivity, ε_λ is the spectral emissivity, α_λ is the spectral absorptivity, G_C is the solar concentration factor and δ is the Delta-Dirac function and 0.73 is a factor to decrease the incident intensity of 1.36 Suns to 1 Suns.

Finally, since the phenomenon of interest is the radiative flux, it will be calculated by integrating the intensity field in all the directions. This is represented in Equation *(3-8)*.

$$q_r = 2\pi\int_0^\infty\int_{-1}^{1} I_\lambda \mu d\mu d\lambda \qquad \textbf{(3-8)}$$

After the radiative flux is obtained, it could be fed as an input to the heat equation to find the temperature profile. However, this will include an iterative procedure, since both fields are treated as independent with this approach, while in reality they are coupled. The heat equation will be given in detail in the next chapter.

3.2.2. Coupled Radiation and Conduction Heat Transfer

After the radiative heat flux is obtained, the effects of conduction inside the insulator and the convective boundary conditions have to be added to the thermal analysis. Moreover, the radiative solution only deals with the inside effects for simplicity arguments. Therefore, the radiation with the surroundings must also be considered here.

For any body, the heat transfer analysis boils down to solving the energy equation, whose general form is given in Equation *(3-9)*. This equation is given in Cartesian coordinates, which is what is used for the analysis described in this study.

$$\rho \frac{DH}{Dt} = \frac{DP}{Dt} + \Phi + \nabla(k\nabla T) - \nabla\left(\sum_{i}^{N} \rho Y_i V_i h_i\right) - \nabla q_r - \dot{q} \qquad \textbf{(3-9)}$$

where D()/D() represents the total derivative. For the optimization purposes, it is assumed that the radiative flux profile, which solved in the previous section, acts as a heat generation term. Moreover, only the steady state solution is sought, and any other heat generation effects are neglected. Finally, the heat flow is assumed to be unidirectional. After these assumptions, the heat equation takes the form given in Equation *(3-10)*.

$$\nabla q_r = k \frac{\delta^2 T}{\delta x^2} \qquad \textbf{(3-10)}$$

The boundary conditions for the heat equation are also given in Equation *(3-11a)*.

$$(k \frac{dT}{dx})_{x=0} = U_{top}(T(x=0) - T_\infty) + \varepsilon(T^4(x=0) - T_\infty^4) \qquad \textbf{(3-11a)}$$

$$(k \frac{dT}{dx})_{x=L} = U(T(x=L) - T_\infty) + \varepsilon(T^4(x=L) - T_\infty^4) \qquad \textbf{(3-12)}$$

Equations *(3-6)*, *(3-8)* and *(3-10)* will be solved simultaneously with the corresponding boundary conditions given in Equations *(3-7a)* and *(3-11a)* in

order to obtain the temperature profile for the optimum insulation case. Numerical methods using iterative procedures were employed for the solutions of these equations for specific parameters. The results are given in Chapter 5.

3.3. Conversion Efficiency

After obtaining the solutions for the insulating plate, it is desired to compare how it performs compared to other insulation techniques. Therefore, a certain form of efficiency needs to be defined. Here, a conversion efficiency is defined, which represents the ratio of the amount of the heat that is transferred into the working fluid in the thermodynamic cycle to the incoming solar flux. Mathematically, this definition is represented in Equation *(3-13)*.

$$\eta = \frac{U(T(x = L) - T_\infty)}{G_C * 1000} \qquad \textbf{(3-13)}$$

where 1000 W/m^2 represents the unit 1 Suns. The denominator is simply the incident radiative solar flux. The results of the conversion efficiencies for different types are given in Chapter 5.

CHAPTER 4: FABRICATION AND EXPERIMENTAL CHARACTERIZATION OF SILICA AEROGELS

Since this study was mainly focused on the design of the optimum silica aerogel based solar insulation system, the next step was to fabricate the aerogels and optimize them according to the needs of the system. After the gels were prepared, they were characterized using different experimental methods in order to observe whether the gels were able to satisfy the requirements for optimum insulation. Finally, the recipes for the aerogels were optimized according to the data that was collected from the experimental methods. This chapter will primarily focus on the fabrication of the silica aerogels and the experimental methods that were exploited in order to characterize the prepared silica aerogels.

4.1. Research Methodology

The aerogels had to be optically transparent to solar spectrum ($0 < \lambda < 2.7$ μm); therefore, recipes that had already been proven to yield transparent aerogels were chosen as the starting points for the fabrication process [47]. After that point, a number of gels were prepared in order to optimize the fabrication process. Due to the fact that silica aerogel preparation is a relatively long process (approximately 3 weeks per gel), this step was chosen as the initial fabrication goal. Furthermore, cracked aerogels were usually observed during this phase, and methods to reduce cracking were also sought.

Another point that needed immediate attendance was the choice of the molds for the aerogels. After trying a number of different candidates such as plastic containers, quartz crucibles and syringes, the syringes were chosen as the best candidates for aerogel fabrication. Syringes were chosen due to the presence of a plunger in them and the flexibility of their use. In fact, the caps were usually cut away after the soon-to-be-gelled chemical solutions were sucked in to make the liquid exchange and gel discharge processes even easier.

After the gels were set for each successful recipe in the syringe molds, the liquid exchange processes were optimized. This included the use of different alcohols and different aging times and frequencies in order to investigate the effects of the aging process. In the end, the use of ethanol was found to be the best amongst methanol, ethanol, isopropyl alcohol (IPA) and acetone. The main reasons for that choice included the best optical transmissivity to solar radiation, the clarity of the gels and the faster drying times. A drying control additive can also be used to balance the stresses that will have to be endured by the gels during the liquid exchange and drying processes. The optimum recipe that was developed in this study includes dimethyl formamide (DMF) as the drying control chemical additive (DCCA).

The next step was to determine the surface polarity of the aerogels; in other words, whether they were in the hydrophilic or the hydrophobic domains. The first finding was that the aerogels were hydrophilic when they were fabricated using conventional methods of aerogel preparation. However, for some applications, which may even include solar insulation, the aerogels might be needed to be hydrophobic. Therefore, methods to make them hydrophobic were also investigated.

The final fabrication step was the drying of the alcogels that were formed when the chemical solution gelled inside the molds in order to evacuate all the liquid inside and replace them by air. The drying could be accomplished subcritically or supercritically. Supercritical drying was chosen as the primary means of drying, while the other methods were also examined. The reasons for this choice will be given in the forthcoming sections of this chapter.

Finally, the best gels for each recipe were experimentally characterized according to their optical characteristics. During this characterization, mainly Ultra violet – Visible (UV-Vis) Spectroscopy was utilized. After the recipes were optimized, the final products were also investigated using the Fourier Transform

Infrared (FTIR) Spectroscopy technique. The final product was also examined in terms of its particle size distribution using a Zetasizer, which makes use of Dynamic Light Scattering (DLS) technique, and density in order to have physical insight on the final produced aerogel.

4.2. Data Collection

The experimental data was collected through the user interface software that the utilized UV-VIS and FTIR spectrometers had built in them. These data were later transferred to a computer and filtered accordingly. Due to the presence of air inside the chambers of the spectrometer and the transparent nature of the aerogels between specific wavelengths, some data were unrealistic. These unrealistic conditions include negative transmissivities at certain wavelengths and or more than 100% transmissivity at others. The experiments were then run using more care, and some methods were applied in order to filter out the unrealistic data.

The data for the particle size distribution were collected using the built in interface the Zetasizer had. The software already had a filtering function in itself; thus, there was no need this time to filter the data.

The density of the final product was measured using conventional techniques. First, the mass of the aerogel was measured using a precision scale. Then, the volume of the aerogel was measured using non-destructive techniques. If the gel was hydrophobic, the utilized technique was to use a graduated cylinder filled with water. If the gel was hydrophilic; however, the use of water would be destructive. Therefore, the volumes of the hydrophilic gels were calculated through geometric measurements. In the end, the density was calculated from their ratio.

More information about the experimental techniques that were utilized along with their working principles will be given in the forthcoming sections of this chapter.

4.3. Fabrication

In this section, the steps of silica aerogel fabrication will be given in detail along with the used recipes and their iterations.

4.3.1. Utilized Silica Aerogel Recipes

Although there are numerous ways to fabricate a silica aerogel, this study mainly focused on tetremethyl orthosilicate (TMOS) and tetraethyl orthosilicate (TEOS) based aerogels due to their fast gelation times, ease of use and low costs. These base materials, also known as silicate sources, are then diluted with the respective alcohols and through the addition of a catalyst to speed up a process, the skeleton chemical solution is formed. This solution is then poured into molds and let sit for a certain amount of time to obtain the gels. The solution also may or may not contain a DCCA in order to balance the stresses that are faced during the liquid exchange and drying steps.

The recipes that were developed and investigated are given in this section.

4.3.1.1. First Recipe

The first recipe that was followed was obtained from another source and was TMOS based [48]. It used TMOS, methanol as the diluent agent and a special catalyst, which was also utilized in all the forthcoming TMOS based recipes. The catalyst was a NH_4OH (ammonium hydroxide) + H_2O (water) mixture with a 5.4 ml ammonium hydroxide by 1000 ml water ratio.

The molar ratio of the recipe was 0.01:1:4.12:7.38 (NH_4OH:TMOS:H_2O:MeOH). The gels were formed in an average of 23 minutes under ambient room conditions (approximately 72 °F and 50% relative humidity). The gels usually had cracks during the drying process, and they were not optically good enough for the purposes of this study. Therefore, they had to be improved. A gel of the first recipe is depicted in Figure 4-1. An Aerogel of Recipe 1

4.3.1.2. Second Recipe

The second recipe was a modification of the first one. To improve the transparency to solar radiation, the molar ratio of TMOS to methanol was decreased from 1:7.3 to 1:8. The total molar ratio of the recipe was 0.01:1:4.47:8 (NH_4OH:TMOS:H_2O:MeOH) and the average forming time was 27 minutes under ambient room conditions (approximately 72 °F and 50% relative humidity). These gels also had cracks during the drying processes and had to be improved.

4.3.1.3. Third Recipe

Again, this recipe was a modification of the first and the second ones. In fact, only the molar ratio of TMOS to methanol was changed from 1:8 to approximately 1:12 to have better transparency. The total molar ratio of the recipe was 0.017:1:6.71:12.14 (NH_4OH:TMOS:H_2O:MeOH) and the average forming time was 35 minutes under ambient room conditions (approximately 72 °F and 50% relative humidity). Most of these gels also had cracks during the drying processes and had to be improved; however, some gels dried with reasonable amounts of cracks and hence they could be used for research purposes. A gel of this recipe is depicted in Figure 4-2. An Aerogel of Recipe 3

4.3.1.4. Fourth Recipe

This recipe was a TEOS based one and it was also adopted from the literature as a starting point and modified a little bit [49]. It used TEOS, ethanol as the diluent agent and a special catalyst. The catalyst was a NH_4OH (ammonium hydroxide) + NH_4F (ammonium fluoride) + H_2O (water) mixture with a 18.35 ml ammonium fluoride by 227.8 ml ammonium hydroxide by 1000 ml water ratio.

The molar ratio of the recipe was 0.00661:0.077:1:16.703:17.955 (NH_4F: NH_4OH:TEOS:EtOH:H_2O). The gels were formed in an average of 83 minutes under ambient room conditions (approximately 72 °F and 50% relative humidity). The forming time of the gels were too long, and the transparencies were significantly lower than the TMOS based aerogels; therefore, TEOS gels were not considered as the optimum materials for the purposes of this study and they were not reiterated.

4.3.1.5. Fifth Recipe

This recipe was the optimized version of the third one, with the addition of DMF as the DCCA. The DMF acts as a controller for the pore size distributions and stresses, which helps keep the gel intact and reduce the cracking incidents. The molar ratio of the gel was approximately the same as the third recipe with the addition of DMF, 0.017:0.091:1:6.71:12.23 (NH_4OH:DMF:TMOS:H_2O:MeOH). The gelation time on average was 45 minutes under ambient room conditions (approximately 72 °F and 50% relative humidity).

This recipe reduced the number of cracked aerogels significantly and produced gels that were suitable for the purposes of this study. Therefore, this recipe was used as the optimum one. A gel of this recipe is depicted in Figure 4-3. An Aerogel of Recipe 5. Although the optical transparencies of the gels could further be increased by playing with the molar ratios, especially the molar ratio of

TMOS to methanol, it also results in drastically increased gelation times and was not considered for this study.

4.3.2. Liquid Exchange

The alcogel that is prepared is very brittle in nature, and its solid structure is not uniform. In order to atone for that, the gel is kept in a pure alcohol for a certain amount of time. During this time, the alcohol diffuses into the gel and settles in the pores. It also acts as a binder for the solid skeleton of the gel and lets the silica form a better solid matrix in there by giving them much more time to form their bonds. It also inhibits the drying process of the alcogel by keeping it wet all the times.

The liquid exchange should be performed for a specific amount of time, with certain amounts of refreshed alcohols and using a specific alcohol which can be determined experimentally. In this study; methanol, ethanol, IPA and acetone were used as the exchange agents. Acetone changed the color of the gels from a bluish glazing alcogel to a yellowish tone. Moreover, its optical properties were not as good as the other candidates. Therefore, it was eliminated from considerations after the first iterations. Although IPA, methanol and ethanol did not yield significant changes in the optical properties, ethanol was the best and was chosen as the primary exchange agent for the purposes of this study. Moreover, ethanol has the best miscibility with liquid carbon dioxide amongst these three agents. This was another reason why ethanol was chosen as the agent, since a higher miscibility with carbon dioxide should also make the supercritical drying faster.

As for the refreshment frequency and exchange times, the golden rule that was found was the more you exchange the gel into a pure alcohol, the denser the gel is going to be. However, the denser the gel is, the more conductive and the less transparent it becomes. Hence, it was an optimization process. In the end, the procedure that was found to be effective was exchanging the gel into ethanol for

21 days inside the syringe mold with refreshments every 24 hours for a fifth recipe based alcogel of 4 mL. Naturally, if the exchange is performed outside the mold, this time should be less, as the diffusion process will be much faster due to the lack of area limitations for the alcohol to penetrate into the gel. Likewise, if the volume of the gel is less, this time will also be less.

Liquid exchange is an essential part of the aerogel fabrication process and must be performed with care.

4.3.3. Hydrophobic Treatment

This is an optional process that is performed only if the end product that is wanted for a specific application is a hydrophobic aerogel. Hydrophobicity by definition represents non-polar molecules that are repelled by water [50]. These aerogels tend to be more durable, as they repel water molecules in the air and their solid structures are not affected by the water vapor molecules in humid air. Moreover, what is also found is that their optical transmissivities to solar radiation are also higher than the hydrophilic aerogels of the same recipe. The reason for that can be attributed to the lack of hydroxyl bonds in these types of structures, which minimizes the hydroxyl stretching absorption in specific wavelength bands [45]. However, their infrared transmissivities are also higher due to the same reason; thus, whether a hydrophilic or a hydrophobic aerogel is better for solar insulation purposes is an optimization problem.

The way to achieve hydrophobicity in an aerogel is through dehydrating it and roughening the surface. In order to dehydrate the alcogel, several methods and materials can be utilized. The agents that were considered in this study were trimethyl chlorosilane (TMCS) and hexamethyldisilazane (HMDS). These agents should be diluted in pure alcohols and for each one the used alcohols were hexane and ethanol, respectively.

Although there are numerous ways to perform this process, the ones that were considered for this study were kept simple. A solution consisting of 1:9 volume ratio of hydrophobe agent to alcohol were prepared for each, and the alcogels were soaked into those solutions for specific amounts of times. In the end, it was seen that HMDS based solution gave better results in terms of optical properties and hydrophobicity and it was chosen as the primary hydrophobe agent. For the HMDS, the procedure was similar to the liquid exchange part. The gel was soaked in the solution for a week with changes every 24 hours inside the syringe mold for a fifth recipe based alcogel of 4 mL. After completion of this process, the gel was soaked into ethanol for three days with refreshments every 12 hours to prepare it for the supercritical drying process.

The hydrophobic treatment results in a more durable aerogel that repels water and this gel can be used for insulation under various conditions.

4.3.4. Drying of the Alcogels

After the alcogels are prepared and aged, they should be dried to obtain the final solid product called the aerogels. Since the solid matrix of the aerogels are not strongly bonded and there exists millions of pores in the aerogels, the drying process should be performed with extreme care. Otherwise, the gels will be cracked. The drying will be finalized when all the liquid inside the alcogel is replaced by air. This is accomplished by evaporating the liquid inside and draining it out. After that, air fills in to the pores and the aerogel is obtained. This drying could be obtained subcritically or supercritically.

4.3.4.1. Subcritical Drying

Subcritical drying refers to the drying of the aerogels that are performed below the critical point of the constituents, mainly the alcohol inside the gel, which is ethanol in our case. This could include drying under ambient conditions, freeze drying and pinhole drying methods.

4.3.4.1.1. Drying under Ambient Conditions

The alcogels can be dried under ambient conditions (approximately 72 °F and 50% relative humidity). On the other hand, this usually results in cracked and shattered aerogels which are not very useful for solar insulation purposes. In fact, ambient drying of hydrophilic aerogels results in solid aerogel powders. Unless an aerogel powder is sought, the hydrophilic aerogels should never be dried in ambient conditions.

The hydrophilic gels, though, being more resilient and durable than the hydrophilic ones, can be dried under ambient conditions. The end results are aerogels that are crack free; however, these gels also shrink in volume and become much less transparent to solar radiation due to increased densities. If the evaporation rate can somehow be controlled, though, the shrinkage can be controlled and useful aerogels can be obtained.

For the purposes of this study, ambient drying was not considered.

4.3.4.1.2. Freeze Drying

The freeze drying is a good way to avoid the liquid gas meniscus in order to evacuate the liquid inside. This method also is a good way to avoid the shrinkage of the volume during evaporation and the stresses endured by the alcogels in the meanwhile. This results in less number of cracks in the aerogels [51]. However, the alcogels are also prone to thermal stresses that can be endured due to rapid temperature changes, and therefore, this method might initiate other problems in the aerogels. Therefore, although it is a good and easy way to avoid the meniscus, this method was not considered for the purposes of this study.

4.3.4.1.3. Pinhole Drying

Another ingenious technique that was developed in the last decade was the drying of the alcogels through pinhole drying method. In this method, the alcogel

is placed in a container which is filled with ethanol. Then, the container is sealed and the ethanol is evaporated. Care must be given, though, not to boil the ethanol since it will result in stresses on the alcogels which might result in cracks or even fractures. After the room is filled by ethanol vapor, pinholes on the surface that are predetermined in size are opened and the container is placed in a controlled environment in which temperature and humidity changes are negligible. Then, the ethanol in the chamber is slowly replaced by air for a specific amount of time. This results in a controlled evaporation rate and results in minimum number of cracks. There still is volume shrinkage, though, and the density of the alcogel increases; however, it does not really affect the optical properties by much. Therefore, it is a really good way to dry the aerogels. The pinhole drying may be combined with supercritical drying to yield the best results [52, 53]. On the other hand, pinhole drying was not considered for the purposes of this project.

4.3.4.2. Supercritical Drying

The most prominent method to dry the alcogels is the supercritical drying. In this technique, the alcogel is placed in a pressurized vessel. The critical point can be done in two ways; with an ethanol critical point dryer or a carbon dioxide critical point dryer. In the ethanol critical point dryer, the alcogel is taken above the critical point of ethanol (T = 514 K, P = 63 bar) [54]. However, the temperature for this is too large and the critical point dryers that do that are rather expensive. Thus, researchers mainly utilized the carbon dioxide critical point dryer due to the lower critical temperature (T = 304.1 K, P = 73.8 bar) [36]. The phase diagram of carbon dioxide is given in Figure 4-4. Phase Diagram of Carbon Dioxide [55].

The working principle of a carbon dioxide critical point dryer is simple. The material is placed inside a vessel along with a specific amount of alcohol. The alcohol should be the alcohol that is present inside the alcogel, which is ethanol

in our case. Then, the chamber is sealed and pressurized, and liquid carbon dioxide is allowed in. The liquid carbon dioxide then mixes with the ethanol. The mixture of ethanol and carbon dioxide is then drained out using a valve, while liquid carbon dioxide is also filled in. This process is called purging. After it is made sure that no more ethanol is coming out, the drainage valve is closed and the sample is left in liquid carbon dioxide for a period of time. For this process, the longer the sample sits in liquid carbon dioxide, the less ethanol it is going to possess in the structure; therefore, the solution should be exchanged into carbon dioxide for a sufficient amount of time. This time depends on the volume and the alcohol content of the alcogel, as well as its geometry. Moreover, the operation temperature and pressures for purging and exchange into liquid carbon dioxide are also important. The optimum operation temperature and pressure are found to be 10°C and 800 psi, respectively.

The purging and exchange into liquid carbon dioxide should be carried a number of times. For our project, it was found that three purge and two exchanges were optimal. After these processes, the heater is turned in and the temperature and pressure is allowed to go above the critical point. When the critical point is reached and passed, a timer is set and the sample is let in there for a period of time. Although this time also depends on the volume and geometry of the alcogel, usually no more than 60 minutes is required. This time is required because all the carbon dioxide inside the alcogel should reach supercritical fluid phase.

The final stage of supercritical drying is depressurizing. The alcogel that now contains supercritical carbon dioxide inside should be depressurized at constant temperature to avoid the meniscus and go down to the gas phase without forming the meniscus. However, since the solid structure of the alcogel is not strong, depressurizing too fast might also result in fractured aerogels. Therefore, the depressurizing should also be performed in lower rates. In fact, the optimum depressurizing rate was found to be 80 psi/min. After the ambient pressure is reached, the aerogel is obtained through supercritical drying of the alcogel.

For the purge and solvent exchange, some empirical equations were developed making use of the experience gained through fabrication of numerous aerogels under different conditions. These equations are developed for the fifth recipe; however, they should work for most of the aerogels since the alcohol content of our fifth recipe is much greater than it is on normal aerogels. Equation *(4-14)* gives the time in minutes for the first purging stage. Here, the amount of ethanol that is used should not be less than 7 mL, no matter how small the sample is. Moreover, there should be enough ethanol to cover the surface of the sample. Therefore, the amount of ethanol that is initially placed in the vessel should be recorded and given as an input for Equation *(4-14)*. Equation *(4-15)* shows the time in minutes for the second and third purging stages. Equation *(4-16)* shows the time in minutes for the first and second solvent exchange processes. For equations *(4-14)* through *(4-16)*, the volumes of the gels and ethanol are in milliliters.

$$t_{p1} = \frac{V_{eth}}{7} \times 10 \qquad \textbf{(4-14)}$$

$$t_{p,i} = C_i V_{gel} \qquad \textbf{(4-15)}$$

Where for the second purge i = 2 and C_2= 2 min/mL and for the third purge i=3 and C_3= 1.5 min/mL.

$$t_{se,i} = C_i \frac{V_{gel}}{30} \qquad \textbf{(4-16)}$$

Where for the first solvent exchange i =1 and C_1= 720 min and for the second solvent exchange i=2 and C_2= 240 min.

These equations constitute the base to determine the periods of time in which purging and solvent exchange are performed.

4.4. Experimental Characterization

After the aerogel is synthesized, its properties should be determined in order to validate if the synthesized gel is useful for the solar thermal insulation applications. The properties that should be characterized include the transmissivity and absorptivity spectrum, density, particle size distribution, pore size distribution and thermal conductivity. For the purposes of this study, pore size distribution and thermal conductivity are not considered.

4.4.1. Experimental Characterization of Density

Silica aerogel is one of the most low density solids that have ever been manufactured [20]. The characterization of density is important in order to verify the high optical transparency and low thermal conductivity of the aerogel. The thermal conductivity is linked directly to density of the solid through a linear relation, and the optical transparency is linked to the arrangement and content of the silica particles, which in turn also determine the density of the material. Thus, investigating the density gives an idea of the range of the optical transparency and thermal conductivity.

In order to find the densities, traditional methods had been utilized. First, the mass of the aerogel was measured using a precision scale. Then, the volume of the aerogel was measured using non-destructive techniques. If the gel was hydrophobic, the utilized technique was to use a graduated cylinder filled with water. If the gel was hydrophilic; however, the use of water would be destructive; therefore, the volume of the hydrophilic gels were calculated through geometric measurements. In the end, the density was calculated from Equation *(4-17)*.

$$\rho_{gel} = \frac{m_{gel}}{V_{gel}} \qquad \textbf{(4-17)}$$

4.4.2. Experimental Characterization of Particle Size Distribution

The characterization of particle size distribution is important for several reasons. These reasons include, but are not limited to the fact that the investigation of the particle size distribution in a material gives valuable information about the homogeneity of the material, and the fact that the distributions and the average particle sizes can be used to estimate the physical and chemical properties of a substance, which also include the optical properties.

In order to characterize the particle size distribution of the aerogels, dynamic light scattering (DLS) technique was utilized through a Zetasizer machine.

4.4.2.1. Dynamic Light Scattering

Dynamic light scattering (DLS) is a technique in which the particle size distribution of the material that is under investigation is imaged by the change in polarization states of an incident monochromatic light due to scattering by the particles in that material. The main idea is to determine the fluctuations of the light due to Rayleigh scattering and diffraction that is a result of scattering and change of polarization states. In Rayleigh scattering, the particles scatter in all directions diffusely and this phenomenon occurs when the wavelength of the light is comparable to the particle sizes of the material; therefore, this technique is really efficient in imaging small particle sizes (<≈250 nm).

Since the exposure to light also excites some of the particles, the intensity of scattered light fluctuates in time and these fluctuations cause interference phenomenon to take place. Then, by analyzing these physical phenomena

correctly through some specific correlations, the DLS method estimates the particle size distributions and the mean effective diameter of particles.

DLS is used in various fields including nanotechnology, physics, biology and mechanical engineering.

4.4.3. Experimental Characterization of Optical Properties

Since the ultimate goal of this project is to find a material that would lead to optimum solar insulation, the most important characterization aspect is the optical properties; namely optical transmissivity. The aerogel mainly consists of pores and silica; thus, at lower wavelengths ($0 < \lambda < \sim 900$ nm) the main optical extinction mechanism is Rayleigh scattering; so reflection dominates in these regions. After that region, absorption starts to happen. Since these regions are conveniently distinguished, only looking at the transmissivity data is enough. In order to obtain the transmissivity data of the prepared samples, light spectroscopy techniques; mainly UV-Vis and FTIR spectroscopy methods had been utilized.

This section will shed light on the operating principles of the two aforementioned light spectroscopy techniques.

4.4.3.1. Ultra Violet – Visible (UV-Vis) Spectroscopy

UV-Vis spectroscopy refers to transmission spectroscopy in the ultra violet or visible region. There is usually a monochromatic light source which is incident on a surface whose optical properties are examined. There is also a reference beam with the exact same configurations. Both beams are then collected in identical sensors which are located across the light source, and the differences in the light intensities and directions are analyzed. This analysis gives the transmissivity of the material that is under investigation. The ranges the UV-Vis spectrometers cover are usually from 200 nm to 2.5 μm [56].

4.4.3.2. Fourier Transform Infra Red (FTIR) Spectroscopy

FTIR technique is a spectroscopy technique in which the infrared absorptivities, or emissivities of the surfaces are examined. There is again a light source which is incident upon the surface whose optical properties are examined. In FTIR, data is simultaneously collected instead of collecting single wavelength data at a time. This makes them much faster than normal dispersive IR spectrometers. Furthermore, it also keeps the signal to noise ratio at a higher level along with the fact that FTIR makes use of interferometers rather than monochromators. Another advantage of FTIR over conventional dispersive monochromatic spectrometers is that the use of the interferometer allows it to have more stable wavelength measurements. This stability is then in turn converted into more resolution by optimizing the design procedures.

FTIR makes use of Fourier transformations in order to convert the data into spectrum ranges. This gives it its name of Fourier Transform IR Spectroscopy. The range of an FTIR is usually from 2.5 to approximately 20 μm [57].

4.5. Figures

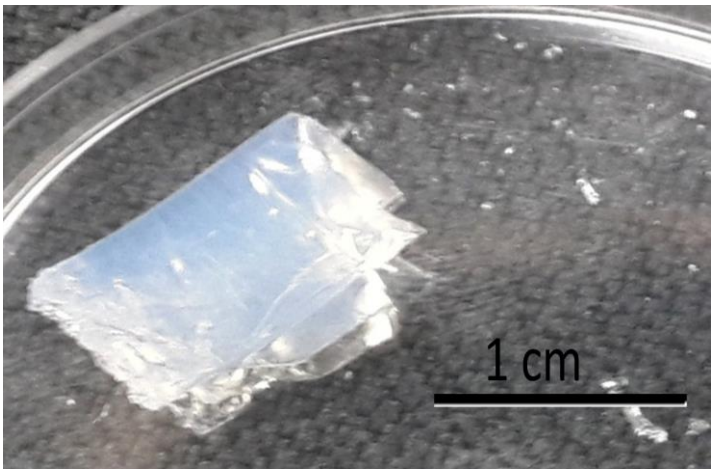

Figure 4-1. An Aerogel of Recipe 1

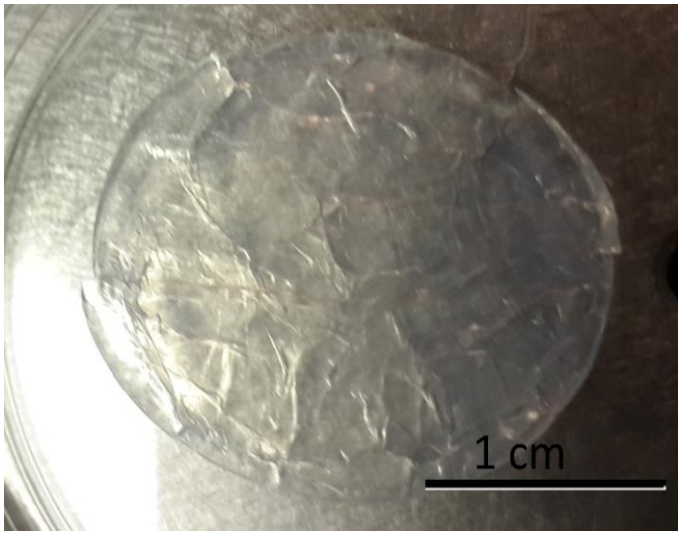

Figure 4-2. An Aerogel of Recipe 3

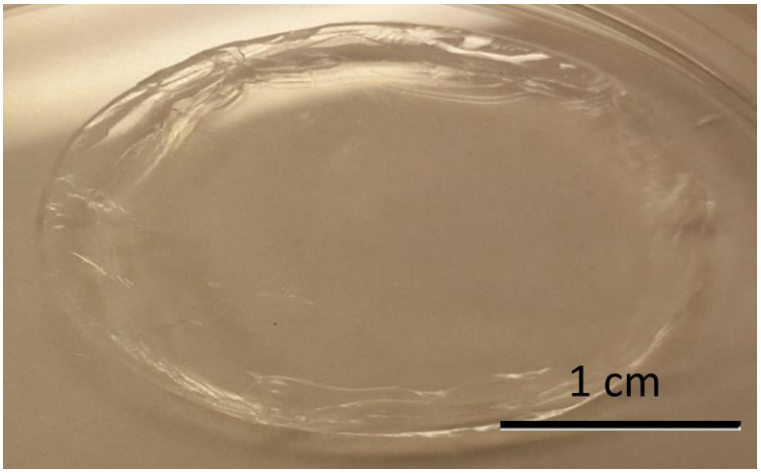

Figure 4-3. An Aerogel of Recipe 5

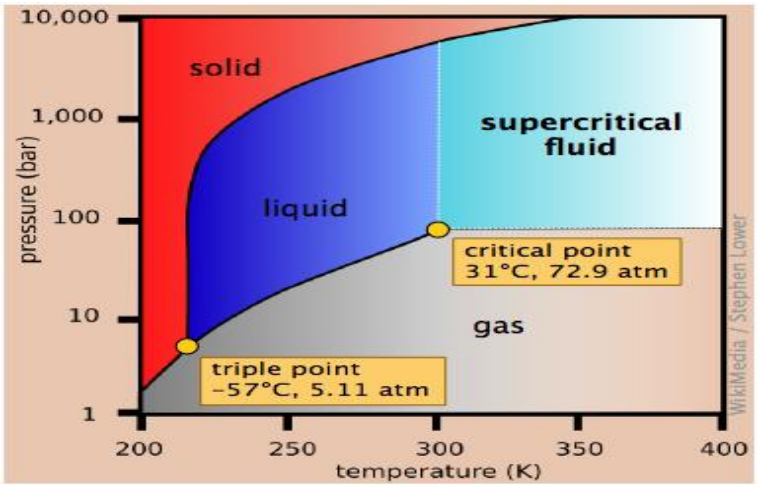

Figure 4-4. Phase Diagram of Carbon Dioxide. Adapted from Ref [55].

CHAPTER 5: RESULTS AND DISCUSSION

The results of the numerical solutions that were described in Chapter 3 and the experimental procedures that were described in Chapter 4 will be given here in detail. First, the results of the numerical thermal model will be given and discussed in detail. Then, the experimental results will be given and the outcomes will be investigated.

5.1. Modeling Results and Discussion

In this section, the results of the developed numerical model are given. First, the expected temperature profiles from the numerical solutions will be investigated. Then, the meanings of these profiles will be explained through the conversion efficiency phenomenon.

5.1.1. Temperature Profiles

The numerical solutions for the theory given in Section 3.2.1 and in Section 3.2.2 were mainly interested in getting the temperature profiles inside the OTTI layer. The analyses were run for a thermal conductivity of k=0.005 W/mK, an OTTI layer thickness of L=4 mm, an overall heat transfer coefficient of U_{top}=10 W/m^{2}K for the top surface (x=0), an overall heat transfer coefficient of U=100 W/ W/m^{2}K for the bottom surface (x=L) and different solar concentration factors of G_C=1, 5, 10, 15 and 20. In other words, the radiative incident heat fluxes were q_r= 1 Suns, 5 Suns, 10 Suns, 15 Suns and 20 Suns, respectively. Finally, the ambient temperature was assumed to be the same as the fluid temperature in the heat exchanger, and the value was T_∞=300 K. Also, the assumptions included τ_λ = 1 for solar spectrum ($0 \leq \lambda \leq 2.7$ μm) and ε_λ = 1 for the Infra-Red emission spectrum (2.7 μm $\leq \lambda \leq \infty$). This means that the optimum OTTI layer with perfect transparency to solar radiation and perfect absorption to emission from the absorbing surface is modeled.

The profiles were solved using an iterative scheme. First, the radiative transfer equation (Equation *(3-6)*) was solved with the corresponding boundary conditions given in Equation *(3-7a)*. Then, the intensity field was integrated numerically to get the flux, in accordance with Equation *(3-8)*. After getting the radiative heat flux, it was numerically differentiated to get its divergence. Finally, the divergence of the radiative flux was fed into Equation *(3-10)*, which was solved to satisfy the boundary conditions given in Equation *(3-11a)*. This process was continued till the defined error margin on the corresponding temperatures was kept below a certain increment, which was chosen to be 0.0001 K. The results are given in Figure 5-1. Temperature Profiles for five Different Solar Concentrations for OTTI Layer Insulation

Examining Figure 5-1. Temperature Profiles for five Different Solar Concentrations for OTTI Layer Insulation, the first thing that needs to be realized is that the temperature values go up for increasing values of G_C, as expected. The temperature increase at the bottom surface is much more pronounced than the increase at the top surface, which means the insulation is working pretty well. In fact, if the curve representing the case when G_C=1 is compared to the case when G_C=20, it is seen that while the temperatures for the bottom surface are T_{bot} = 307 K for G_C=1 and T_{bot} = 475 K for G_C=20; the temperatures for the top surface are T_{top} = 306 K for G_C=1 and T_{top} = 340 K for G_C=20. This means that the difference in temperatures for the bottom surface is ΔT_{bot} = 168 K, and for the top surface it is ΔT_{top} = 34 K. This shows that the OTTI layer is really effective in insulation of the solar absorber.

When Figure 5-1. Temperature Profiles for five Different Solar Concentrations for OTTI Layer Insulation is further examined, it is seen that there is a maximum temperature that is occurring inside the OTTI layer itself, rather than on the absorber. This is due to the fact that the emissive losses by the absorber are trapped on the OTTI layer, which are completely absorbed, and then fed back to the absorber itself. The OTTI layer also emits and conducts the trapped

energy upwards, which results in thermal losses from the absorber at the bottom. Therefore, the maximum temperature takes place inside the insulating layer.

Another striking fact that is seen if Figure 5-1. Temperature Profiles for five Different Solar Concentrations for OTTI Layer Insulation is examined is that the location of the maximum temperature shifts downwards, i.e. closer to the absorber, when the solar concentration increases. This happens because the modeled OTTI layer is a very good insulator and emitter. As the temperature of the absorber rises due to the increased heat flux on it, the temperature difference between the maximum temperature in the OTTI layer and the absorber temperature also rises. This results in increased radiative and conductive transport between the bottom of the OTTI layer and the absorber. This transport is enough to keep the emission and conduction upwards at a reasonable level; so the maximum temperature shifts down, since the transport from the OTTI layer that is moving upwards is getting less and less significant.

The temperature profiles clearly show that OTTI layers are promising candidates for optimum solar insulation. The next section will deal with the comparison of this technique to the current insulation techniques.

5.1.2. Conversion Efficiencies

Although the temperature profiles for the OTTI layer simulation give good signs for optimum insulation of solar energy harnessing, they do not tell anything about whether this technique will be better than the current state-of-the-art insulation techniques. Therefore, an efficiency analysis has to be performed. For that, the conversion efficiency that was defined in Chapter 3 and given by Equation *(3-13)* was employed. For that solution, the temperature values that were obtained by the numerical solution described in Section 5.1.1 were used. Here, only the solar concentrations of G_C = 5, 10, 15 and 20 were used; as for 1 suns none of the methods perform much better than the case without insulation.

The investigated cases were insulation by optimum OTTI layers developed in this study, absorption & emission by selective surfaces and insulation by vacuum tubes, and no insulation. The results are given in Table 5-1. The Conversion Efficiencies for three Different Insulation Cases with Different Incident Solar Flux Values

Examining Table 5-1. The Conversion Efficiencies for three Different Insulation Cases with Different Incident Solar Flux Values, it is seen that for all the cases, the optimum OTTI layer insulation performed much better in terms of the conversion efficiency. This is due to the fact that although the selective surfaces absorb much of the heat that come towards them and emit too less, there is a limit to what they can do. In the case of an OTTI layer, the heat that is escaping the absorbing surface is trapped and fed back, creating a continuous source of reheating. Therefore, this effect makes the OTTI layers more effective.

If Table 5-1. The Conversion Efficiencies for three Different Insulation Cases with Different Incident Solar Flux Values is further examined, it is seen that for increasing values of G_C, the efficiencies decrease. This is due to the fact that emissive losses have a quartic dependence on the temperature values; meaning when the temperature gets higher, the emissive loss gets higher much faster. Thus, it is expected that the efficiency values go down as the solar conversion factors go up. This fact is realized in all the considered cases, as expected.

By looking at the simulation results, it can clearly be concluded that OTTI layers have the potential to take over selective surface and vacuum tube combinations in terms of solar thermal insulating systems, since they are more effective in insulating. However, insulating materials that represent absorbing behavior in the Far Infra-Red and transmissive behavior in the Visible and Near Infra-Red regimes have to be developed. This problem will be attended in the next section by investigating the use of optimized silica aerogels.

5.2. Experimental Results and Discussion

The procurement, synthesis and optimization procedures for the silica aerogels were given in Chapter 4. Here, the results of the experimental procedures to characterize silica aerogels in terms of their optical properties, densities and particle size distributions are given in detail. First, the spectroscopy results will be analyzed. Then, the densities will be calculated and showed. Finally, the particle size distributions will be discussed.

5.2.1. Spectroscopy Results

As discussed in Chapter 4, the optical properties of the synthesized silica aerogels were experimentally characterized by making use of light spectroscopy; specifically UV-Vis Light Spectroscopy and FTIR Spectroscopy. The results of the individual analyses were given here in detail. Moreover, at the end of the section, the combined analysis is also given to give better visualization.

5.2.1.1. UV-Vis Spectroscopy Results

The aerogels were characterized for their optical spectral properties falling in the Ultraviolet, Visible and Near Infra-Red regimes (0.2 μm ≤ λ ≤ 2.5 μm) using the UV-Vis spectrometer. The analyses were performed in high resolution and the noises were filtered out. Three different aerogels were characterized and their UV-Vis spectroscopy results are given in Figure 5-2. UV-Vis Spectral Transmissivity Data for three Different AerogelsThe characterized three different aerogels were; a commercially available transparent hydrophilic aerogel which was fabricated by Aerogel Technologies, an optimized synthesized transparent hydrophilic aerogel (Recipe 5) and an optimized synthesized transparent hydrophobic aerogel (Recipe 5) of the same thickness of L = 4 mm.

If Figure 5-2. UV-Vis Spectral Transmissivity Data for three Different Aerogels is examined, it is seen that up to λ = 650 nm, the transmissivities of the silica

aerogels are rising. This is due to the fact that there is a significant amount of Rayleigh scattering in that regime. For the hydrophilic gels, this effect is more pronounced, as the hydrophobic one starts to rise faster due to carrying much less amounts of water inside it.

The second thing to realize is that when the spectral transmissivities are stabilized at a constant value for a band of wavelengths, the hydrophilic ones exhibit better transparency than the hydrophobic one. This can be explained by the fact that the hydrophobic aerogel is a denser material with a stronger solid structure, which decreases transparency. This fact will be revisited in Section 5.2.2.

Another thing to realize is that the spectral transmissivities are very high for the hydrophilic aerogels from λ = 650 nm to λ = 1350 nm, λ = 1500 nm to λ = 1850 nm and λ = 1950 nm to λ = 2100 nm. Furthermore, the spectral transmissivities are also very high for the hydrophobic aerogel from λ = 550 nm to λ = 2100 nm for the hydrophobic gel unceasingly. The reason for the dips that are observed in the hydrophilic ones is that there are bands of absorption for water in the vicinity of λ = 1380 nm and in the vicinity of λ = 1870 nm [45]. In these bends, the O-H bonds that the water has start to stretch and vibrate, resulting in tremendous amounts of absorption of the incident light. Since the hydrophilic ones still contain some amount of water and hydroxyl bonds at the surface, they suffer from decreased transmissivities in the vicinity of the bands. For the hydrophobic aerogel, that is not a huge problem, as it contains significantly less amounts of water due to the hydrophobic treatment it received. The effects of these dips can be decreased by dehydrating the aerogels more rigorously.

Furthermore, it is also seen from Figure 5-2. UV-Vis Spectral Transmissivity Data for three Different Aerogels that in the vicinity of λ = 2.34 μm, all three of the samples exhibit a decrease in transmissivity. This is also due to the fact that carbon monoxide has a band in the vicinity of λ = 2.34 μm, and it reduces the

transmissivity due to excessive absorption by carbon monoxide molecules. This time, even the hydrophobic one suffers from it, because it contains similar amounts of carbon monoxide in itself as the hydrophilic ones.

Finally, after 2.4 μm, there is an abrupt decrease in the transmissivities in the hydrophilic aerogels. This is again due to the fact that there is a water band in the vicinity of λ = 2.7 μm, which is much stronger than the other bands. The band at λ = 2.7 μm is in fact called a fundamental band, in which absorption is even more important. This fact will be investigated in more detail in the forthcoming section.

When these results are examined, it is seen that silica aerogels exhibit pretty good transmissivities in the UV-Vis spectroscopy regime. It can further be concluded that the hydrophobic aerogels exhibit a better transparency to solar radiation than the hydrophilic ones due to decreased Rayleigh scattering and O-H stretching effects.

5.2.1.2. FTIR Spectroscopy Results

After completing the UV-Vis spectroscopy, the FTIR spectroscopy was also performed in order to investigate the performances of silica aerogels in the Far Infra-Red regime of interest (2.5 μm $\leq \lambda \leq$ 12.5 μm). The analyses were again done in high resolutions and the noises were filtered out. The same three aerogels were characterized as in Section 5.2.1.1. The spectral transmissivity data for the FTIR spectrum is given in Figure 5-3. FTIR Spectral Transmissivity Data for three Different Aerogels

The first thing to realize while looking at Figure 5-3. FTIR Spectral Transmissivity Data for three Different Aerogels is that the transmissivities decrease rapidly to 0 in the vicinity of λ = 2.7 μm and stay at 0 until λ = 3.5 μm. This is due to the fact that at λ = 2.7 μm, the bands of silica, water and carbon dioxide overlap. Silica and water have their fundamental bands at λ = 2.7 μm,

meaning very strong absorption, and carbon dioxide has a C-O stretching band. Thus, the effects of the band overlap go on for a broad range of wavelengths, keeping the transparency at 0% and absorption at a 100%.

The second thing to realize from Figure 5-3. FTIR Spectral Transmissivity Data for three Different Aerogels is that between λ = 3.5 μm and λ = 5 μm, there is some transmission of light, which is much more pronounced in the hydrophobic aerogel. For the hydrophilic ones, the water's molecular vibrations keep the absorption at higher levels, resulting in decreased transparency, while for the hydrophobic one, due to lack of water molecules, there is a significant amount of transmission.

Another thing to realize between the same wavelength range is that in the vicinity of λ = 4.3 μm, there is a big dip in the transmissivities. This is caused by the fundamental band of carbon dioxide that is present at that wavelength. Additionally, water also has a band in the vicinity of λ = 4.7 μm, which pulls the transmissivities for the hydrophilic aerogels at 0% without affecting the hydrophobic one significantly.

Finally, after λ = 5μm, the silica is absorbing and there is no further transmission, meaning complete absorption.

If these results are examined, it is clearly seen that silica aerogels exhibit a good absorptive behavior in the FTIR wavelength range (Near Infra-Red). This time, the hydrophilic aerogels are much more absorptive in the FTIR wavelength range.

5.2.1.3. Combined Results

The combined spectroscopy measurements are given in Figure 5-4. Combined UV-Vis and FTIR Spectral Transmissivity Data for three Different Aerogelsin order to give better visualization. Moreover, the spectrally averaged

transmissivities of the three aerogels of interest are given in the first row of Table 5-2. Summary of Experimental Characterization for three Different Characterization Aspects and Three Different AerogelsBy inspecting this table, it is seen that the synthesized aerogels perform much better than the commercially available one in terms of transparency to solar radiation. Moreover, the fact that the hydrophobic gel is a better transmitter of solar radiation is also justified, due to the higher optical transmissivity value.

By looking at Figure 5-4. Combined UV-Vis and FTIR Spectral Transmissivity Data for three Different Aerogels, it is seen that although the hydrophobic aerogels are more transparent to solar radiation, they are also less absorptive in the low energy photon regime, meaning emissive losses from the absorbing surface will also be transmitted outwards. On the contrary, although the hydrophilic aerogels are less transparent to solar radiation, they are much more absorptive in the low energy photon regime, meaning they will trap the emissive losses from the bottom surface. Thus, whether a hydrophilic gel is better or vice versa is another optimization process, which is beyond the scope of this study.

5.2.2. Density Characterization Results

The density values for the synthesized aerogels are given in the second row of Table 5-2. Summary of Experimental Characterization for three Different Characterization Aspects and Three Different Aerogels When these values are examined, it is seen that the synthesized aerogels are much less dense than the commercially available aerogel, although all the aerogels are of very low density for solid materials as expected. Additionally, the hydrophilic aerogel performs much better in terms of low density characteristics than the hydrophobic one due to the fact that the hydrophobic treatment fills up the pores with some other chemical compositions which increase the weight of the aerogel, even though the reduced surface tension forces decrease the volume. Thus, the hydrophobic aerogel performs worse than the hydrophilic aerogel when there are no Rayleigh scattering or band absorption effects in terms of transparency.

5.2.3. Particle Size Distribution Results

The average silica particle diameters are given in the third row of Table 5-2. Summary of Experimental Characterization for three Different Characterization Aspects and Three Different Aerogels Here, the commercially available gel could not be characterized since it could not fit in the chamber of the Zetasizer.

When the average particle sizes are examined, it is seen that they are in the order of 1 nm. This shows that silica aerogels that were synthesized were actually made of nanoparticles connected by pores. This is really important in understanding the optical and physical properties, and it actually helps explain why the synthesized aerogels have high transparencies and low densities.

5.3. Figures

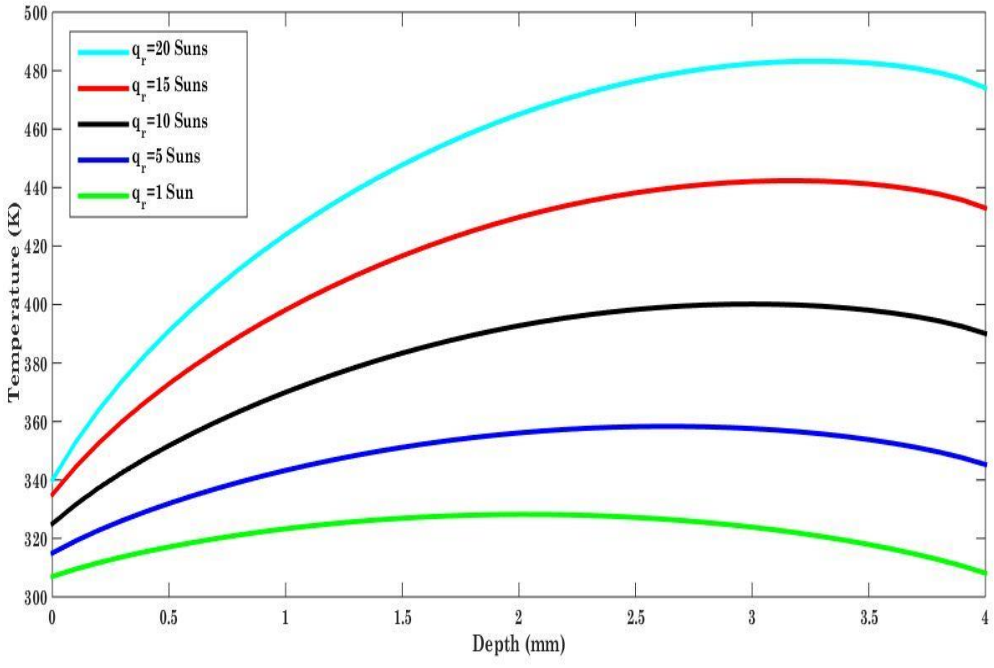

Figure 5-1. Temperature Profiles for five Different Solar Concentrations for OTTI Layer Insulation

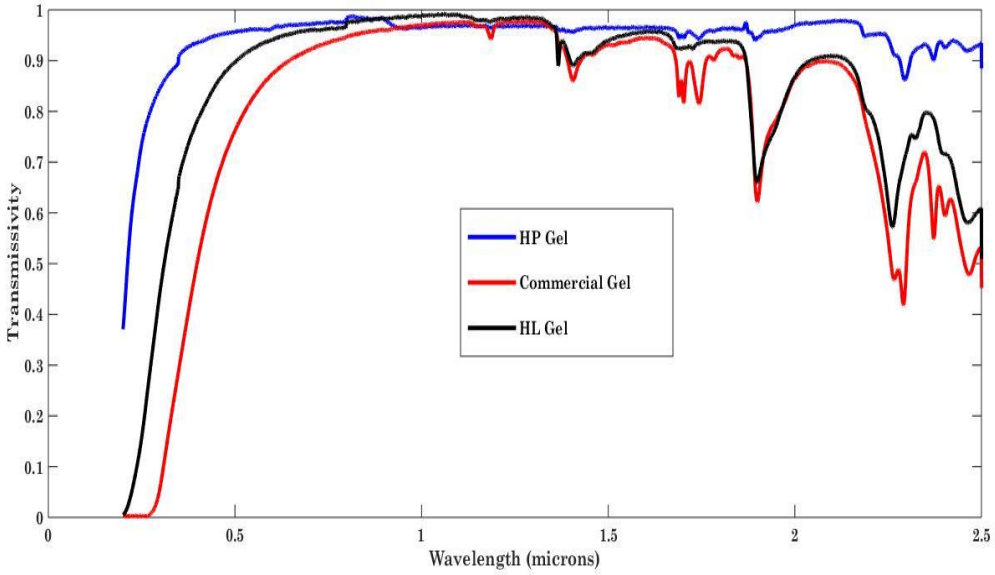

Figure 5-2. UV-Vis Spectral Transmissivity Data for three Different Aerogels

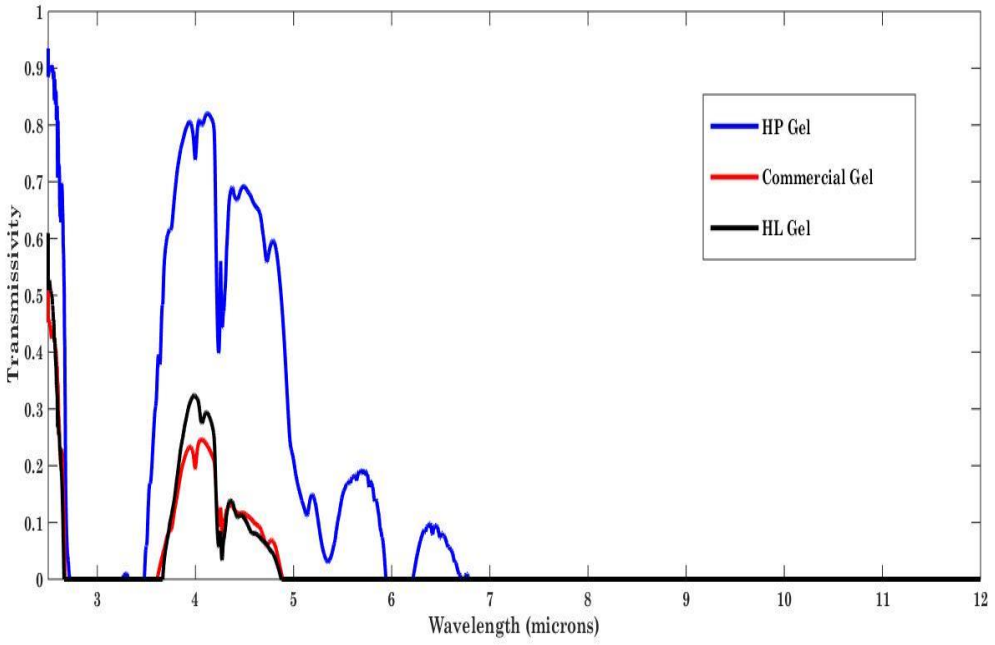

Figure 5-3. FTIR Spectral Transmissivity Data for three Different Aerogels

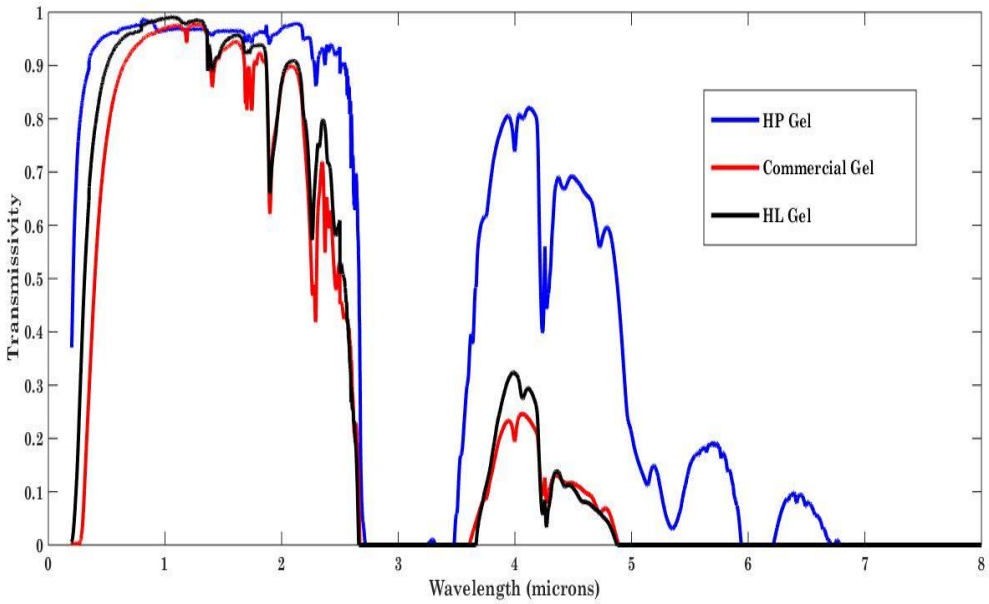

Figure 5-4. Combined UV-Vis and FTIR Spectral Transmissivity Data for three Different Aerogels

5.4. Tables

Table 5-1. The Conversion Efficiencies for three Different Insulation Cases with Different Incident Solar Flux Values

G_C	η without Insulation	η for Selective Surface & Vacuum Tube	η for optimized OTTI Layer
5	0.802	0.830	0.905
10	0.780	0.820	0.900
15	0.763	0.800	0.887
20	0.741	0.780	0.870

Table 5-2. Summary of Experimental Characterization for three Different Characterization Aspects and Three Different Aerogels

Characterized Aspect	*Synthesized Hydrophilic Gel*	*Synthesized Hydrophobic Gel*	*Commercial Gel (Hydrophilic)*
Spectrally Averaged Transmissivity	0.87	0.95	0.80
Average Particle Diameter (nm)	0.9	0.9	-
Density (kg/m^3)	29.8	146.5	170.8

CHAPTER 6: CONCLUSION

In conclusion, this study investigated whether utilizing an OTTI layer for solar thermal insulation directly on top of any kind of broadband absorber would function well in terms of minimizing the thermal losses from the system. The proposed system was simulated numerically to get the temperature profiles in the insulation, the final temperature of the absorber and the amount of heat that is transferred to the working fluid. The results were compared to the prominent insulation method of selective surface & vacuum tube systems and the case of no insulation. Moreover, the use of silica aerogels as OTTI materials was also investigated by procuring, synthesizing and optimizing the silica aerogels and characterizing their physical properties.

By looking at the results of this study, it can be deduced that since the OTTI layers create a heat trapping effect on the system, they perform much better than selective surface and vacuum tube systems in terms of minimizing thermal losses. This fact can be seen by looking at the increased conversion efficiencies. Thus, it can be concluded that OTTI layers have the potential to replace the existing insulation techniques.

Another conclusion to draw from the results of this study is that silica aerogels have the potential to perform the optimum OTTI duties, which were investigated in this study. They cannot be made to have perfect transparency to solar radiation, or perfect opacity to thermal emission from the surfaces; however, they have very high percentages of solar transparency and Infra-Red opacity, which can still further be improved. Since adjusting these usually means decreasing the thermal conductivity, silica aerogels become the perfect OTTI layers for solar insulation. Thus, silica aerogels can definitely be used as a replacement for the current insulation techniques for solar thermal energy.

6.1. Recommended Future Studies

For the experimental part, it could be good to further optimize the aerogel recipes by decreasing the molar ratio of silica with respect to the alcohol in the gel procurement process. This could end up giving an aerogel which has even more transparency and less density. Moreover, a vapor sorption analysis on the aerogels to get the pore size distributions and thermal conductivity measurements in order to have exact values would complete the fabrication part of the aerogels.

As noted in Chapter 5, hydrophobic aerogels had better transparency to sunlight; however, their Infra-Red absorptions were lower. Nanoplasmonic materials could be doped on the aerogels in order to increase their absorptivities in the Infra-Red regime. However, this is an optimization process as it will also have a negative effect on the transparency to solar radiation. Thus, this could also be an interesting optimization study.

The next step in the modeling part would be to model the radiative behavior of silica aerogels directly by also including non-perfect transparencies to solar radiation in the Ultraviolet, Visible and Near Infra-Red regime and non-perfect emissivities in the Far Infra-Red regime to get the exact behavior.

Finally, experimental validations on the obtained results for the proposed solar energy harnessing system could be sought with the help of a solar simulator with a setup to measure the temperature values at specific locations on the aerogels and on the absorbing plate.

REFERENCES

[1] U.S. Energy Information Administration. Annual energy review 2011. Technical report, Department of Energy / Energy Information Administration, 2012.

[2] Grant W Petty. *A first course in atmospheric radiation*. Sundog, 2004.

[3] M Reim, W Körner, J Manara, S Korder, M Arduini-Schuster, H-P Ebert, and J Fricke. Silica aerogel granulate material for thermal insulation and daylighting. *Solar Energy*, 79(2):131–139, 2005.

[4] Karsten I Jensen. Passive solar component based on evacuated monolithic silica aerogel. *Journal of non-crystalline solids*, 145:237–239, 1992.

[5] Svend Svendsen. Solar collector with monolithic silica aerogel. *Journal of non-crystalline solids*, 145:240–243, 1992.

[6] John A Duffie and William A Beckman. *Solar engineering of thermal processes*, volume 3. Wiley New York etc., 1980.

[7] Brian Norton. *Harnessing Solar Heat*. Springer, 2014.

[8] Charles Kittel and Herbert Kroemer. *Thermal physics*. Macmillan, 1980.

[9] Martin A Green. Solar cells: operating principles, technology, and system applications. 1982.

[10] Matthew Buresch. Photovoltaic energy systems: Design and installation. 1983.

[11] Solar Energy , Retrieved April 18 , 2016 Retrieved from: https://www3.epa.gov/climatechange/kids/solutions/technologies/solar.html.

[12] William Shockley and Hans J Queisser. Detailed balance limit of efficiency of p-n junction solar cells. *Journal of applied physics*, 32(3):510–519, 1961.

[13] Eden Rephaeli and Shanhui Fan. Absorber and emitter for solar thermo-photovoltaic systems to achieve efficiency exceeding the shockley-queisser limit. *Optics express*, 17(17):15145–15159, 2009.

[14] Soteris A Kalogirou. Solar thermal collectors and applications. *Progress in energy and combustion science*, 30(3):231–295, 2004.

[15] GL Morrison, I Budihardjo, and M Behnia. Water-in-glass evacuated tube solar water heaters. *Solar energy*, 76(1):135–140, 2004.

[16] E. Hecht. *Optics*. Pearson education. Addison-Wesley, 2002.

[17] Yen-Po Chen, Ching-Tao Li, and Likarn Wang. Single-crystalline silicon solar cell with selective emitter formed by screen printing and chemical etching method: A feasibility study. *International Journal of Photoenergy*, 2013, 2013.

[18] OP Agnihotri and Brijen K Gupta. Solar selective surfaces. 1981.

[19] Mehmet Esen. Thermal performance of a solar cooker integrated vacuum-tube collector with heat pipes containing different refrigerants. *Solar Energy*, 76(6):751–757, 2004.

[20] Michel A Aegerter, Nicholas Leventis, and Matthias M Koebel. *Aerogels handbook*. Springer Science & Business Media, 2011.

[21] A Soleimani Dorcheh and MH Abbasi. Silica aerogel; synthesis, properties and characterization. *Journal of materials processing technology*, 199(1):10–26, 2008.

[22] M Schmidt and F Schwertfeger. Applications for silica aerogel products. *Journal of non-crystalline solids*, 225:364–368, 1998.

[23] Aerogels: Thinner, Lighter, Stronger (July 28, 2011) Retrieved April 18, 2016. Retrieved from: http://www.nasa.gov/topics/technology/features/aerogels.html.

[24] John CC Fan, Frank J Bachner, George H Foley, and Paul M Zavracky. Transparent heat-mirror films of tio2/ag/tio2 for solar energy collection and radiation insulation. *Applied Physics Letters*, 25(12):693–695, 1974.

[25] ND Kaushika and K Sumathy. Solar transparent insulation materials: a review. *Renewable and sustainable energy reviews*, 7(4):317–351, 2003.

[26] Claes G Granqvist. *Materials science for solar energy conversion systems*, volume 1. Elsevier, 2013.

[27] M Reim, A Beck, W Körner, R Petricevic, M Glora, M Weth, T Schliermann, J Fricke, Ch Schmidt, and FJ Pötter. Highly insulating aerogel glazing for solar energy usage. *Solar Energy*, 72(1):21–29, 2002.

[28] J Fricke and T Tillotson. Aerogels: production, characterization, and applications. *Thin Solid Films*, 297(1):212–223, 1997.

[29] Jochen Fricke and Andreas Emmerling. Aerogels. *Journal of the American Ceramic Society*, 75(8):2027–2035, 1992.

[30] S Henning and L Svensson. Production of silica aerogel. *Physica Scripta*, 23(4B):697, 1981.

[31] Jyoti L. Gurav, In-Keun Jung, Hyung-Ho Park, Eul Son Kang, and Digambar Y. Nadargi. Silica aerogel: Synthesis and applications. *J. Nanomaterials*, 2010:23:1–23:11, January 2010.

[32] Lawrence W Hrubesh and John F Poco. Thin aerogel films for optical, thermal, acoustic and electronic applications. *Journal of non-crystalline solids*, 188(1):46–53, 1995.

[33] Lawrence W Hrubesh. Aerogel applications. *Journal of Non-Crystalline Solids*, 225:335–342, 1998.

[34] Douglas M Smith, Alok Maskara, and Ulrich Boes. Aerogel-based thermal insulation. *Journal of non-crystalline solids*, 225:254–259, 1998.

[35] J Fricke, X Lu, P Wang, D Büttner, and U Heinemann. Optimization of monolithic silica aerogel insulants. *International journal of heat and mass transfer*, 35(9):2305–2309, 1992.

[36] MJ Van Bommel and AB De Haan. Drying of silica aerogel with supercritical carbon dioxide. *Journal of Non-Crystalline Solids*, 186:78–82, 1995.

[37] Sheng Dai, YH Ju, HJ Gao, JS Lin, SJ Pennycook, and CE Barnes. Preparation of silica aerogel using ionic liquids as solvents. *Chem. Commun.*, (3):243–244, 2000.

[38] H Yokogawa. hydrophobic silica aerogel. *Handbook of sol-gel science and technology*, 3:73–84, 2005.

[39] CJ Lee, GS Kim, and SH Hyun. Synthesis of silica aerogels from waterglass via new modified ambient drying. *Journal of Materials Science*, 37(11):2237–2241, 2002.

[40] AR Buzykaev, AF Danilyuk, SF Ganzhur, EA Kravchenko, and AP Onuchin. Measurement of optical parameters of aerogel. *Nuclear Instruments and Methods in Physics Research Section A: Accelerators, Spectrometers, Detectors and Associated Equipment*, 433(1):396–400, 1999.

[41] GM Pajonk. Transparent silica aerogels. *Journal of Non-Crystalline Solids*, 225:307–314, 1998.

[42] Zhongsheng Deng, Jue Wang, Aimei Wu, Jun Shen, and Bin Zhou. High strength sio 2 aerogel insulation. *Journal of non-crystalline solids*, 225:101–104, 1998.

[43] G Herrmann, R Iden, M Mielke, F Teich, and B Ziegler. On the way to commercial production of silica aerogel. *Journal of non-crystalline solids*, 186:380–387, 1995.

[44] Theodore L Bergman, Frank P Incropera, and Adrienne S Lavine. *Fundamentals of heat and mass transfer*. John Wiley & Sons, 2011.

[45] M Quinn Brewster. *Thermal radiative transfer and properties*. John Wiley & Sons, 1992.

[46] Andrej Lenert and Evelyn N Wang. Optimization of nanofluid volumetric receivers for solar thermal energy conversion. *Solar Energy*, 86(1):253–265, 2012.

[47] Recipes for making Silica Aerogel. (n.d.) Retrieved from: http://www.aerogel.org/?cat=51.

[48] Silica Aerogel (TMOS-Base Catalyzed) (n.d.) Retrieved from: http://www.aerogel.org/?p=1406.

[49] A Venkateswara Rao and Sharad D Bhagat. Synthesis and physical properties of teos-based silica aerogels prepared by two step (acid–base) sol–gel process. *Solid State Sciences*, 6(9):945–952, 2004.

[50] Van P Carey. *Liquid-vapor phase-change phenomena*. Hemisphere, New York, NY (United States), 1992.

[51] GM Pajonk, M Repellin-Lacroix, S Abouarnadasse, J Chaouki, and D Klavana. From sol-gel to aerogels and cryogels. *Journal of Non-Crystalline Solids*, 121(1-3):66–67, 1990.

[52] Makoto Tabata, Ichiro Adachi, Yoshikazu Ishii, Hideyuki Kawai, Takayuki Sumiyoshi, and Hiroshi Yokogawa. Development of transparent silica aerogel over a wide range of densities. *Nuclear Instruments and Methods in Physics Research Section A: Accelerators, Spectrometers, Detectors and Associated Equipment*, 623(1):339–341, 2010.

[53] Ichiro Adachi, Makoto Tabata, Hideyuki Kawai, and Takayuki Sumiyoshi. Study of transparent silica aerogel with high refractive index. *Nuclear Instruments and Methods in Physics Research Section A: Accelerators, Spectrometers, Detectors and Associated Equipment*, 639(1):222–224, 2011.

[54] Sang-Do Yeo, Su-Jin Park, Jin-Woo Kim, and Jae-Chang Kim. Critical properties of carbon dioxide+ methanol,+ ethanol,+ 1-propanol, and+ 1-butanol. *Journal of Chemical & Engineering Data*, 45(5):932–935, 2000.

[55] 7.5: Changes of state, 2013. http://chemwiki.ucdavis.edu/Textbook_Maps/General_Chemistry_Textbook_Maps/Map%3A_Chem1_(Lower)/07%3A_Solids_and_Liquids/7.05%3A_Changes_of_State.

[56] Heinz-Helmut Perkampus, Heide-Charlotte Grinter, and TL Threlfall. *UV-VIS Spectroscopy and its Applications*. Springer, 1992.

[57] Peter R Griffiths and James A De Haseth. *Fourier transform infrared spectrometry*, volume 171. John Wiley & Sons, 2007.